144	PRKACB	1	NM_001242858	c.C738G	p.F246L	nonsynonymous SNV	-	-	-	-	-	-	-	-	-	-	-	-	-	-	○	-	-	-	-	-
145	PRKACG	9	NM_002732	c.G565A	p.A189T	nonsynonymous SNV	-	-	-	-	-	-	-	-	-	-	-	-	○	-	-	-	-	-	-	-
146	PRKCQ	10	NM_006257	c.A428G	p.H143R	nonsynonymous SNV	-	-	-	-	-	○	-	-	-	-	-	-	-	-	-	-	-	-	-	-
147	PRKCZ	1	NM_002744	c.A295C	p.T99P	nonsynonymous SNV	-	-	-	-	-	-	-	○	-	-	-	-	-	-	-	-	○	-	-	-
148	PTK2	8	NM_153831	c.3127_3131del	p.1043_1044del	frameshift deletion	-	-	-	-	-	○	-	-	-	-	-	-	-	-	-	-	-	-	-	-
149	RET	10	NM_020630	c.G1588A	p.E530K	nonsynonymous SNV	-	○	-	-	-	-	-	-	-	-	-	-	-	-	-	-	-	-	-	-
150	RIPK4	21	NM_020639	c.C2296G	p.L766V	nonsynonymous SNV	-	-	-	-	-	-	-	-	-	-	-	-	○	-	-	-	-	-	-	-
151	RNASEL	1	NM_021133	c.G1823A	p.R608Q	nonsynonymous SNV	-	-	○	-	-	-	-	-	-	-	-	-	-	-	-	-	-	-	-	-
152	RPS6KA1	1	NM_002953	c.T214G	p.S72A	nonsynonymous SNV	-	-	○	-	-	-	-	-	-	-	-	-	-	-	-	-	-	-	-	-
153	RPS6KB2	11	NM_003952	c.G1264A	p.V422I	nonsynonymous SNV	-	○	-	-	-	-	-	-	-	-	-	-	-	-	-	-	-	-	-	-
154	RPS6KC1	1	NM_001136138	c.A2204G	p.K735R	nonsynonymous SNV	-	-	-	-	-	-	-	-	○	-	-	-	-	-	-	-	-	-	-	-
155	SCYL1	11	NM_001048218	c.G163A	p.E55K	nonsynonymous SNV	-	-	○	-	-	-	-	-	-	-	-	-	-	-	-	-	-	-	-	-
156	SCYL2	12	NM_017988	c.T767C	p.M256T	nonsynonymous SNV	-	-	-	-	-	-	-	-	-	○	-	-	-	-	-	-	-	-	-	-
157	SGK2	20	NM_016276	c.A923C	p.H308P	nonsynonymous SNV	-	○	-	-	-	○	○	○	-	○	○	-	-	○	○	○	-	-	-	○
158	SIK1	21	NM_173354	c.G1888A	p.A630T	nonsynonymous SNV	-	-	-	-	-	-	-	-	-	-	-	-	○	-	-	-	-	-	-	-
159	SRPK1	6	NM_003137	c.G1427A	p.G476E	nonsynonymous SNV	-	-	○	-	-	-	-	-	-	-	-	-	-	-	-	-	-	-	-	-
160	STK10	5	NM_005990	c.G2753A	p.R918Q	nonsynonymous SNV	-	-	-	-	-	-	-	-	-	-	-	-	-	-	○	-	-	-	-	-
161	STK17B	2	NM_004226	c.A304T	p.N102Y	nonsynonymous SNV	○	-	-	-	-	-	-	-	-	-	-	-	-	-	-	-	-	-	-	-
162	STK24	13	NM_003576	c.G310A	p.D104N	nonsynonymous SNV	-	-	-	-	-	-	-	-	-	-	-	○	-	-	-	-	-	-	-	-
163	STK4	20	NM_006282	c.G350A	p.R117Q	nonsynonymous SNV	-	-	-	-	-	-	-	-	-	○	-	-	-	-	-	-	-	-	-	-
164	STK40	1	NM_032017	c.769_770del	p.257_257del	frameshift deletion	-	-	-	-	-	-	-	-	-	-	-	-	○	-	-	-	-	-	-	-
165	STYK1	12	NM_018423	c.A91G	p.T31A	nonsynonymous SNV	-	-	-	-	-	-	-	-	-	-	-	-	-	-	○	-	-	-	-	-
166	TBCK	4	NM_001163435	c.G19A	p.A7T	nonsynonymous SNV	-	-	○	-	-	-	-	-	-	-	-	-	-	-	-	-	-	-	-	-
167	TEK	9	NM_000459	c.A880G	p.K294E	nonsynonymous SNV	○	○	○	○	○	○	○	-	○	-	-	○	-	-	-	-	○	○	○	-
168	TEX14	17	NM_031272	c.G3570C	p.Q1190H	nonsynonymous SNV	-	-	-	-	-	-	-	-	-	-	-	-	-	-	○	-	-	-	-	-
169	TGFBR1	9	NM_001130916	c.G856C	p.D286H	nonsynonymous SNV	-	-	-	-	-	-	-	-	-	-	-	-	-	-	-	-	○	-	-	-
170	TNK2	3	NM_001010938	c.C1814T	p.P605L	nonsynonymous SNV	-	-	-	-	-	-	-	-	-	-	-	-	-	-	○	-	-	-	-	-
171	TRIB2	2	NM_021643	c.A494C	p.H165P	nonsynonymous SNV	-	-	-	-	-	-	-	-	-	-	-	-	○	-	-	-	-	-	-	-
172	TRIM28	19	NM_005762	c.C2441T	p.P814L	nonsynonymous SNV	-	-	-	-	-	-	-	-	-	-	-	○	-	-	-	-	-	-	-	-
173	TRIO	5	NM_007118	c.T7775C	p.F2592S	nonsynonymous SNV	-	-	○	-	○	-	-	-	-	-	-	-	-	-	-	○	-	○	-	-
174	TRPM6	9	NM_001177310	c.C3733A	p.P1245T	nonsynonymous SNV	-	-	-	-	-	-	-	-	-	-	-	-	-	-	-	-	-	-	-	○
175	TSSK4	14	NM_174944	c.T311A	p.L104Q	nonsynonymous SNV	-	-	-	-	-	○	-	-	-	-	-	-	-	-	-	-	-	-	-	-
176	TTBK1	6	NM_032538	c.A295G	p.N99D	nonsynonymous SNV	-	-	-	-	○	-	-	-	-	-	-	-	-	-	-	○	-	-	-	-
177	TYK2	19	NM_003331	c.1036_1037insG	p.N346fs	frameshift insertion	○	○	-	○	○	-	-	○	-	-	-	○	○	○	-	○	-	○	-	○
178	TYRO3	15	NM_006293	c.G1135A	p.A379T	nonsynonymous SNV	-	-	-	-	-	-	-	-	-	-	-	-	-	-	-	-	-	-	○	-
179	UHMK1	1	NM_175866	c.C29T	p.A10V	nonsynonymous SNV	-	-	-	-	-	-	-	-	-	-	-	-	-	-	-	○	-	-	-	-
180	ULK2	17	NM_014683	c.2621delA	p.Q874fs	frameshift deletion	-	-	-	-	-	-	-	-	-	-	-	-	-	-	-	○	-	-	-	-
181	ULK4	3	NM_017886	c.G3746A	p.R1249Q	nonsynonymous SNV	-	-	-	-	-	-	-	-	-	-	-	-	-	-	-	-	-	-	-	○
182	VRK2	2	NM_001130481	c.G775A	p.A259T	nonsynonymous SNV	-	-	-	-	-	-	-	-	-	-	-	○	-	-	-	-	-	-	-	-
183	WNK1	12	NM_014823	c.C4468G	p.P1490A	nonsynonymous SNV	-	-	-	-	-	-	-	-	-	-	-	-	-	-	-	-	-	-	-	○
184	WNK2	9	NM_006648	c.G5350A	p.V1784M	nonsynonymous SNV	-	-	-	-	-	-	-	-	-	○	-	-	-	-	-	-	-	-	-	-
185	WNK4	17	NM_032387	c.G2167A	p.E723K	nonsynonymous SNV	-	-	-	-	-	-	-	-	-	-	-	-	-	-	-	-	-	-	○	-
186	YES1	18	NM_005433	c.G271C	p.G91R	nonsynonymous SNV	-	-	-	-	○	-	-	-	-	-	-	-	-	-	-	-	-	-	-	-

[a]The 20 HCC cell lines analyzed were SNU-449, HUH-6, JHH-7, SK-Hep1, JHH-5, C3A, HepG2, JHH-4, huH-1, HLE, SNU-398, SNU-475, HLF, Alexander, KIM-1, JHH-1, JHh-2, SNU-182, SNU-423 and SNU-387.
[b]RefSeq Accession number registered in the National Center for Biotechnology Information (NCBI) database (http://www.ncbi.nlm.nih.gov/sites/entrez?db=gene).
Abbreviation: Chr, chromosome

Supplementary Table S7.
mTOR and MAPK pathway gene alterations in the HCC cell lines

Gene symbol	Alternative name	rsID[a]	RefSeq ID[b]	Chr	Genome position	cDNA	Amino acid	Cell lines																		
								SNU44	HUH6	JHH7	HuH7	SKHep1	JHH5	C3A	HepG2	JHH4	huH1	HLE	SNU39	SNU47	HLF	Alex	KIM1	JHH1	SNU18	SNU42	SNU37
BRAF		rs113488022	NM_004333	7	140453136	c.T1799A	p.V600E	-	-	-	-	○	-	-	-	-	-	-	-	-	-	-	-	-	-	-	-
RPS6KA1	RSK1		NM_002953	1	26873463	c.T214G	p.S72A	-	-	○	-	-	-	-	-	-	-	-	-	-	-	-	-	-	-	-	-
RPS6KA1	RSK1	rs2229712	NM_002953	1	26883511	c.A1004C	p.K335T	-	-	-	-	-	-	-	-	-	○	-	-	○	-	-	-	-	○	-	-
RPS6KA6	RSK4	rs6616890	NM_014496	X	83320017	c.G2074A	p.D692N	○	-	-	-	-	-	-	-	-	-	-	○	○	-	-	○	-	-	-	-
RPS6KB2	S6K2		NM_003952	11	67202161	c.G1264A	p.V422I	-	○	-	-	-	-	-	-	-	-	-	-	-	-	-	-	-	-	-	-
RPS6KB2	S6K2	rs55987642	NM_003952	11	67200812	c.C800T	p.P267L	-	-	-	-	○	-	-	-	○	-	-	-	-	-	-	○	○	-	-	-
RPS6KB2	S6K2	rs13859	NM_003952	11	67202156	c.C1259T	p.A420V	○	○	○	○	○	-	-	-	○	○	-	-	-	-	○	○	○	○	-	-
STK11	LKB1	rs59912467	NM_000455	19	1223125	c.C1062G	p.F354L	-	-	○	-	-	-	-	-	-	-	-	-	○	-	-	-	-	-	-	-

[a]Reference Cluster ID registered in the dbSNP (http://www.ncbi.nlm.nih.gov/projects/SNP/) database (as of March 2013).
[b]RefSeq accession number registered in the NCBI database.
Shaded rows indicate DNA variations not registered as genetic polymorphisms in the dbSNP database.

Supplementary Table S8. Chou-Talalay median dose effect analysis

	1	2	3	4	5
AZD8055 (nM)	**12.5**	**25**	**50**	**100**	**200**
CI-1040 (μM)	**3.75**	**7.5**	**15**	**30**	**60**
Drug Combination Ratio	**1:300**	**1:300**	**1:300**	**1:300**	**1:300**
CI[a]	**0.893**	**0.766**	**0.711**	**0.709**	**0.835**

[a]CI value was calcurated using the CompuSyn software package (ComboSyn, Inc, http://www.combosyn.com). CI = 1, additive effect; CI <1, synergistic effct; CI >1, antagonistic effect.
Abbreviations: CI, combination index.

Supplementary Table S9. List of the MAPK and mTOR signaling components for unsupervised hierarchical clustering analyses

#	Signaling Components	Phosphorylation site(s)	KEGG Pathway[a]	CST Antibody Category
1	p-p53	Ser20	MAPK	DNA damage
2	p-p53	Ser46	MAPK	DNA damage
3	p-p53	Ser15 16G8	MAPK	DNA damage
4	p-p53	Ser37	MAPK	DNA damage
5	p-p53	Ser392	MAPK	DNA damage
6	p-p53	Ser6	MAPK	DNA damage
7	p-p53	Ser9	MAPK	DNA damage
8	p-p53	Ser15	MAPK	DNA damage
9	p-NFkB p65	Ser536	MAPK	NFkB
10	p-NFkB p65	Ser276	MAPK	NFkB
11	p-NFkB p65	Ser468	MAPK	NFkB
12	p-ATF-2	Thr71 11G2	MAPK	p38 MAPK
13	p-HSP27	Ser82	MAPK	p38 MAPK
14	p-MAPKAPK-2	Thr222	MAPK	p38 MAPK
15	p-MAPKAPK-2	Thr2334	MAPK	p38 MAPK
16	p-MKK3/MKK6	Ser189/207	MAPK	p38 MAPK
17	p-MSK1	Thr581	MAPK	p38 MAPK
18	p-p38 MAPK	Thr180/Y182	MAPK	p38 MAPK
19	p44/42 MAP kinase	Thr202/Tyr204	MAPK	Ras-Raf
20	p-CREB	Ser133	MAPK	Ras-Raf
21	p-MEK1/2	Ser217/221	MAPK	Ras-Raf
22	p-Mnk1	Thr197/202	MAPK	Ras-Raf
23	p-p90RSK	Thr359/Ser363	MAPK	Ras-Raf
24	p-p90RSK	Ser380	MAPK	Ras-Raf
25	p-p90RSK	Thr573	MAPK	Ras-Raf
26	p-PAK1	Ser144	MAPK	Ras-Raf
27	p-PAK1	Ser199/204	MAPK	Ras-Raf
28	p-PAK1	Thr423	MAPK	Ras-Raf
29	p-PAK2	Ser20	MAPK	Ras-Raf
30	p-Raf-A	Ser299	MAPK	Ras-Raf
31	p-Raf-b	ser445	MAPK	Ras-Raf
32	p-Raf-c	Ser338	MAPK	Ras-Raf
33	p-Raf-c	Ser289/296/301	MAPK	Ras-Raf
34	p-Raf-c	Ser259	MAPK	Ras-Raf
35	p-RSK	Thr356/Ser360	MAPK	Ras-Raf
36	p-RSK2	Ser227	MAPK	PI3K-AKT-mTOR
37	p-EGF Receptor	Tyr1045	MAPK	RTK/TK
38	p-EGF Receptor	Tyr1068	MAPK	RTK/TK
39	p-EGF Receptor	Tyr992	MAPK	RTK/TK
40	p-PDGF Receptor-β	Thr1009	MAPK	RTK/TK
41	p-PDGF Receptor-β	Thr740	MAPK	RTK/TK
42	p-PDGF Receptor-β	Thr751	MAPK	RTK/TK
43	p-PDGF Receptor-β	Thr771	MAPK	RTK/TK
44	p-PDGF Receptor-β	Thr1021	MAPK	RTK/TK
45	p-ATF-2	Thr71	MAPK	SAPK/JNK
46	p-c-Jun	Ser63	MAPK	SAPK/JNK

47	p-c-Jun	Ser73	MAPK	SAPK/JNK
48	p-SAPK/JNK	Thr183/Y185	MAPK	SAPK/JNK
49	p-SAPK/JNK	Thr183/Tyr185	MAPK	SAPK/JNK
50	p-SEK1/MKK4	Thr261	MAPK	SAPK/JNK
51	p-TAK1	Thr184/187	MAPK	TGF-β
52	p-AMPKa	Thr172	mTOR	Glucose metabolism
53	p-IRS-1	Ser307	mTOR	Glucose metabolism
54	p-IRS-1	Ser612	mTOR	Glucose metabolism
55	p-IRS-1	Ser636/639	mTOR	Glucose metabolism
56	p-LKB1	Ser428	mTOR	Glucose metabolism
57	p-PKC(pan)βII	Ser660	mTOR	Phospholipase
58	p-PKCα/β	Thr638/641	mTOR	Phospholipase
59	p-4E-BP1	Thr70	mTOR	PI3K-AKT-mTOR
60	p-4E-BP1	Thr37/46	mTOR	PI3K-AKT-mTOR
61	p-4E-BP1	Ser65	mTOR	PI3K-AKT-mTOR
62	p70-S6 kinase	Thr389	mTOR	PI3K-AKT-mTOR
63	p-Akt	Thr308	mTOR	PI3K-AKT-mTOR
64	p-eEF2k	Ser366	mTOR	PI3K-AKT-mTOR
65	p-elF4B	Ser422	mTOR	PI3K-AKT-mTOR
66	p-elF4E	Ser209	mTOR	PI3K-AKT-mTOR
67	p-elF4G	Ser1108	mTOR	PI3K-AKT-mTOR
68	p-GSK-3a	Ser21	mTOR	PI3K-AKT-mTOR
69	p-GSK-3a/β	Ser21/9	mTOR	PI3K-AKT-mTOR
70	p-GSK-3β	Ser9	mTOR	PI3K-AKT-mTOR
71	Phospho-Akt	Ser473	mTOR	PI3K-AKT-mTOR
72	p-mTOR	Ser2448	mTOR	PI3K-AKT-mTOR
73	p-PDK1	Ser241	mTOR	PI3K-AKT-mTOR
74	p-PKD/PKCm	Ser744/748	mTOR	PI3K-AKT-mTOR
75	p-PKD/PKCm	Ser916	mTOR	PI3K-AKT-mTOR
76	p-PRAS40	Thr246	mTOR	PI3K-AKT-mTOR
77	p-PTEN	Ser380	mTOR	PI3K-AKT-mTOR
78	p-Raptor	Ser792	mTOR	PI3K-AKT-mTOR
79	p-S6Rb	Ser235/236	mTOR	PI3K-AKT-mTOR
80	p-S6Rb	Ser240/244	mTOR	PI3K-AKT-mTOR
81	p-Tuberin/TSC2	Ser939	mTOR	PI3K-AKT-mTOR
82	p-Tuberin/TSC2	Thr1462	mTOR	PI3K-AKT-mTOR
83	p-Tuberin/TSC2	Thr1571	mTOR	PI3K-AKT-mTOR

Abbreviations: CST, Cell Signaling Technology, Inc. (Danvers, MA)

[a]The MAPK and mTOR signaling components were selected based on KEGG pathway maps (http://www.genome.jp /kegg/kegg3a.html) and used for unsupervised hierarchical clustering analyses.

Supplementary Table S10. Fisher's exact test: Association of cancer types with activation status of the MAPK and mTOR signaling

	A[a]	B[b]	*P* value (fisher's exact test)
HCC	11	12	0.011
Ovarian Cancer	3	12	0.753
Gastric Cancer	3	12	0.753
Colon Cancer	2	7	1.000
Pancreatic Cancer	2	7	1.000
Osteosarcoma	0	8	0.109
Lung Cancer	3	5	0.416
Oral Cancer	0	7	0.185

[a,b] A and B indicate the subgroups shown in Supplementary Fig.2.

Cancer Science
The official journal of the Japanese Cancer Association JCA

Soluble interleukin-6 receptor is a serum biomarker for the response of esophageal carcinoma to neoadjuvant chemoradiotherapy

Yosuke Makuuchi,[1,2] Kazufumi Honda,[1,10] Yoshiaki Osaka,[2] Ken Kato,[3] Takashi Kojima,[4] Hiroyuki Daiko,[5] Hiroyasu Igaki,[6] Yoshinori Ito,[7] Sumito Hoshino,[2] Shingo Tachibana,[2] Takafumi Watanabe,[1,2] Koh Furuta,[8] Shigeki Sekine,[9] Tomoko Umaki,[1] Yukio Watabe,[1] Nami Miura,[1] Masaya Ono,[1] Akihiko Tsuchida[2] and Tesshi Yamada[1]

[1]Division of Chemotherapy and Clinical Research, National Cancer Center Research Institute, Tokyo; [2]Third Department of Surgery, Tokyo Medical University, Tokyo; [3]Division of Gastrointestinal Oncology National Cancer Center Hospital, Tokyo; [4]Division of Gastrointestinal Oncology, National Cancer Center Hospital East, Kashiwa; Divisions of [5]Radiation Oncology; [6]Esophageal Surgery, National Cancer Center Hospital, Tokyo; [7]Division of Esophageal Surgery, National Cancer Center Hospital East, Kashiwa; [8]Division of Clinical Laboratories, National Cancer Center Hospital, Tokyo; [9]Division of Molecular Pathology National Cancer Center Research Institute, Tokyo, Japan

(Received December 11, 2012/Revised April 25, 2013/Accepted April 27, 2013/Accepted manuscript online May 4, 2013/Article first published online June 13, 2013)

Preoperative chemoradiotherapy has been shown to improve the outcome of patients with esophageal cancer, but because response to this therapy varies, it is desirable to identify in advance individuals who would be unlikely to benefit, in order to avoid unnecessary adverse drug effects. The serum profiles of 84 cytokines and related proteins were determined in 37 patients with esophageal squamous cell carcinoma who received identical neoadjuvant preoperative chemoradiotherapy regimens and underwent surgical resection. Histological response to this therapy was assessed in surgically resected specimens. The serum soluble interleukin-6 receptor (sIL6R) level was significantly higher in 30 patients who failed to achieve a histological complete response ($P = 0.005$). Multivariate analysis revealed that the increased level of sIL6R was one of several significant independent predictors of an unfavorable outcome (hazard ratio, 2.87; $P = 0.017$). The increased level of this cytokine in patients who did not obtain a complete response was reproducibly observed in an independent cohort of 34 patients. Esophageal squamous cell carcinoma patients with an increased serum level of sIL6R are predicted to respond poorly to preoperative chemoradiotherapy, therefore, their exclusion from this treatment may be considered. Persistent systemic inflammation is implicated as a possible mechanism of resistance to this therapy. (*Cancer Sci* 2013; 104: 1045–1051)

Esophageal cancer is one of the leading causes of cancer mortality worldwide, accounting for >300 000 deaths annually.[1] Surgical resection is one of the most reliable methods for local management of the disease, but lymph node metastasis and invasion to neighboring organs, such as the lung, trachea, and large vessels, often hamper curative resection of the tumors. To improve resectability, various trials of PCRT have been attempted,[2–6] and a recent large randomized phase III clinical trial clearly indicated that it improved the overall survival of patients with potentially curable esophageal or esophagogastric-junction cancer.[7]

However, PCRT does not always improve the survival of patients with ESCC. We previously showed an unfavourable outcome of patients with ESCC that did not response to PCRT.[3] Similar results have been reported by other investigators.[8–10] The combination of chemotherapy with radiation enhances the degree of toxicity.[11,12] Therefore, if PCRT proves ineffective, patients potentially would merely have suffered more severe adverse events without receiving any of the anticipated benefits. For this reason, development of a new diagnostic method that would reliably predict the response of every patient to the treatment is clearly desirable.[11]

The biological behavior of cancer may be determined, or at least influenced, by the tissue microenvironment. Cytokine gene expression signatures in non-cancerous tissues have been reported to predict the outcome of patients with hepatocellular carcinoma and lung adenocarcinoma.[13,14] Chemoradiation induces cancer cell death through tumor antigen-specific T-cell responses.[15]

Based on these observations, we assumed that a certain type of host reaction might influence the efficacy of chemoradiotherapy. Here we report the comprehensive profiling of serum cytokines in ESCC patients who received an identical protocol of neoadjuvant PCRT, which revealed a correlation between serum sIL6R and the histological response to PCRT that to our knowledge has not been reported previously.

Materials and Methods

Serum samples. Serum samples from a total of 218 ESCC patients in three retrospective cohorts (PCRT-discovery [$n = 37$], PCRT-validation [$n = 34$], and PCT [$n = 100$]) and two prospective cohorts (prospective PCRT [$n = 26$] and prospective PCT [$n = 21$]) were analyzed.

The diagnosis of primary squamous cell carcinoma was confirmed histologically in all cases by pretreatment endoscopic biopsy. Patients were staged clinically according to the International Union Against Cancer's TNM classification of malignant tumors (6th edition).[16] Serum samples were collected before the initiation of any treatment and kept frozen until analysis. Patients received PCRT (PCRT-discovery, PCRT-validation, and prospective PCRT Cohorts) or preoperative combinational chemotherapy (PCT and prospective PCT Cohorts) and underwent standard esophagectomy and lymphadenectomy with curative intent. Histological responses to treatments were classified into Grades 0–3 (G0, G1, G2, and G3) according to the 9th edition of the Japanese Classification of Esophageal Cancer (Table S1).[17]

Individuals who had previously undergone therapy for esophageal cancer or chemoradiotherapy for other malignancies, or had histories of other active malignancies, were excluded. This study was carried out with approval from the Internal Review Boards on ethical issues of TMU and the

[10]To whom correspondence should be addressed.
E-mail: khonda@ncc.go.jp

doi: 10.1111/cas.12187
© 2013 Japanese Cancer Association

NCC. The therapy protocols used for the various cohorts (1–5) were as follows:

1 PCRT-discovery Cohort was a retrospective cohort of 37 stage II–IVa ESCC patients randomly selected from among those who consecutively received neoadjuvant PCRT at TMU between 2000 and 2005 (Table 1).[3,18] The PCRT consisted of low-dose CDDP (5 mg/m^2/day, 5 days weekly for 4 weeks; total 100 mg/m^2) and 5-FU (350 mg/m^2/day, 5 days weekly for 4 weeks; total 7000 mg/m^2) plus concurrent radiation (10-MV linear accelerator, 2 Gy/day, 5 days weekly for 4 weeks; total 40 Gy). Surgical resection was carried out 4 weeks after the completion of PCRT.

2 PCRT-validation Cohort was a retrospective cohort comprising 34 serum samples obtained from the remaining stage II–III ESCC patients and those who received neoadjuvant PCRT using the same protocol as that for the PCRT-discovery Cohort at TMU between 2006 and 2009 (Table 1).[3,18]

3 Prospective PCRT Cohort was a prospective cohort of serum samples from 26 stage II–III (excluding T4) patients who were enrolled in a phase II clinical trial of neoadjuvant PCRT at the National Cancer Center Hospital and the National Cancer Center Hospital East between 2010 and 2011.[19] These patients underwent two courses of protracted infusion of 5-FU (1000 mg/m^2/day) on days 1–4 and days 29–32, and 2-h infusions of CDDP on days 1 and 29 (75 mg/m^2), along with adequate hydration and antiemetic coverage, plus concurrent irradiation (1.8 Gy/day). Surgical resection was carried out 6–8 weeks after the completion of PCRT.

4 PCT Cohort was a retrospective cohort of serum samples from 100 stage II–III (excluding T4) patients who received neoadjuvant combinational chemotherapy at the NCC between 2003 and 2010. The combinational chemotherapy comprised 5-FU (800 mg/m^2/day) on days 1–5 and days 22–26, and 2-h infusions of CDDP (80 mg/m^2) on days 1 and 22, with adequate hydration and antiemetic coverage. The treatment was repeated three times at 3-week intervals.

5 Prospective PCT Cohort was a prospective cohort comprising serum samples from 21 stage II–III (excluding T4) patients who were enrolled in a phase II clinical trial of neoadjuvant combinational chemotherapy at the National Cancer Center Hospital between 2009 and 2010. The chemotherapy regimen consisted of docetaxel (70 mg/m^2) on day 1, 5-FU (750 mg/m^2/day) on days 1–5, and 2-h infusions of CDDP (70 mg/m^2) on day 1, with adequate hydration and antiemetic coverage. The treatment was repeated three times at 3-week intervals.

Multiplexed immunobead-based assay. The levels of 84 cytokines (listed in Table S2) were measured in the sera of the 37 patients in the PCRT-discovery Cohort using nine multiplex kits: an acute-phase 4-plex panel (Invitrogen, Carlsbad, CA, USA); an SAA human single-plex beads kit (Invitrogen); MAP human serum adipokine panel A (Millipore, Billerica, MA, USA); MAP human serum adipokine panel B (Millipore); MAP human soluble cytokine receptor premix 14-plex (Millipore); the MAP human soluble cytokine/chemokine panel (Millipore); cytokine assay human (Panomics, Fremont, CA, USA); human adhesion molecular multianalyte profile base kit (R&D Systems, Minneapolis, MN, USA); and the human obesity multianalyte profiling kit (R&D Systems). The assays were carried out by investigators who were unaware of the clinical data.

Enzyme-linked immunosorbent assay. The level of serum sIL6R was measured using the ELISA sIL6R assay kit (R&D Systems). The level of c-reactive protein (CRP) was measured using the high-sensitivity ELISA CRP assay kit (Siemens, Munich, Germany). The assays were carried out by investigators who were unaware of the clinical data.

Immunohistochemistry. Formalin-fixed paraffin-embedded biopsy specimens of the prospective PCRT Cohort were cut into 4-μm-thick sections. The sections were immunostained with a rabbit mAb against phosphorylated STAT3 protein at the tyrosine 705

Table 1. Clinicopathological characteristics of esophageal squamous cell carcinoma patients in preoperative chemoradiotherapy (PCRT)-discovery and PCRT-validation cohorts

Variable	PCRT-discovery cohort			PCRT-validation cohort		
	G3 (n = 7)	G2 and G1 (n = 30)	P-value*	G3 (n = 4)	G2 and G1 (n = 30)	P-value*
Age						
<65 years	4 (54%)	21 (70%)	0.66	3 (75%)	14 (47%)	0.60
≥65 years	3 (43%)	9 (30%)		1 (25%)	16 (53%)	
Gender						
Male	5 (71%)	27 (70%)	0.23	4 (100%)	23 (77%)	0.56
Female	2 (29%)	3 (10%)		0	7 (23%)	
Tumor location†						
Ce	0	3 (10%)	0.37	0	1 (3%)	1.00
Te	6 (86%)	27 (90%)		4 (100%)	29 (97%)	
Ae	1 (14%)	0		0	0	
Clinical stage‡						
II	0	4 (13%)	0.30	1 (25%)	3 (10%)	0.41
III	7 (100%)	20 (67%)		3 (75%)	27 (90%)	
IVa	0	6 (20%)		0	0	
CRP§						
<0.3 mg/dL	4 (57%)	15 (52%)	0.57			
≥0.3 mg/dL	3 (43%)	14 (48%)				

Histological responses graded (G1–G3) according to the Japanese Classification of Esophageal Cancer (9th edition). *P-values were calculated using Fisher's extact t-test. †Tumor location was classified according to the Guidelines for Clinical and Pathologic Studies on Carcinoma of the Esophagus (9th edition).[17] ‡Clinical stage was classified according to the International Union Against Cancer's TNM Classification of Malignant Tumors (6th edition).[16] §C-reactive protein (CRP) data were not available for one patient. Ae, Abdominal esophagus; Ce, cervical esophagus; PCRT, preoperative chemoradiotherapy; Te, thoracic esophagus.

doi: 10.1111/cas.12187
© 2013 Japanese Cancer Association

(Y705) residue (Cell Signaling Technology, Boston, MA, USA), as described previously.[18,20]

Statistical analysis. Survival curves covering the period from the date of surgery to the date of death or last follow-up were plotted using the Kaplan–Meier method, and differences between the curves were assessed with the log–rank test. Student's *t*-tests and the Cox proportional hazards regression model were carried out using the StatFlex statistics package (version 5.0) (Atiteck, Osaka, Japan) and tools available in the R statistical package (http://www.r-project.org/).[18,21,22] Differences having *P*-values of <0.05 were considered to be statistically significant.

Results

Circulating cytokines associated with response to PCRT. The levels of 84 cytokines in serum samples from 37 patients that were obtained prior to PCRT (PCRT-discovery Cohort) were measured using the multiplexed immunobead-based assay. All of the patients received the same protocol of chemoradiotherapy (CDDP plus 5-FU and concurrent irradiation) and underwent esophagectomy. Histological examination of the resected specimens revealed that viable tumor cells had completely disappeared in seven (19%) patients (pathological complete response or G3), whereas residual viable tumor cells were detected in the remaining 30 (G1 or G2). No case was graded as G0 (no recognizable effect). There was no significant difference in age, gender, tumor location, clinical stage, or serum CRP level between these two sets of 7 and 30 patients (Table 1). The seven patients who obtained a G3 response showed a markedly favorable postsurgical outcome in comparison with the G1 and G2 cases ($P = 0.014$, log–rank test) (Fig. 1a).

Through multiplex protein profiling we found that the baseline serum levels of six cytokines, including MIP1B ($P = 0.002$, *t*-test), sIL6R ($P = 0.005$), MIP1A ($P = 0.027$), insulin ($P = 0.031$), interferon-α2 ($P = 0.048$), and MMP3 ($P = 0.049$), were significantly decreased in the seven patients who showed a complete pathological response (Table 2). The differences did not remain statistically significant after Bonferroni adjustment for multiple testing,[23] probably due to the small number of patients assessed, especially those who obtained a G3 response.

Correlation coefficient analysis revealed no significant mutual association (correlation coefficient ≥0.70) among the six cytokines (Table S3).

Association of high sIL6R with poorer OS. To further select the most critical factor, the 37 patients in the PCRT-discovery Cohort were classified into two groups according to their levels of each cytokine, and OS was compared between the groups. Among the six cytokines, we found that only the serum level of sIL6R was significantly associated with patient outcome. Nineteen patients with sIL6R higher than 20.5 ng /mL (median value for 37 patients) had significantly worse OS than the remaining 18 ($P = 0.008$, log–rank test) (Fig. 1b). We adopted here the median values for the 37 patients in order to avoid introducing any selection bias.

Univariate analysis by the Cox proportional hazards model (Table 3) revealed that only clinical stage (specifically, stages III–IV *vs* stage II; hazard ratio, 3.06; $P = 0.008$) and serum sIL6R (>20.5 ng/mL *vs* ≤20.5 ng/mL; hazard ratio, 3.20; $P = 0.008$) were significantly correlated with patient outcome. Multivariate analysis indicated that sIL6R (hazard ratio, 2.87; $P = 0.017$) and clinical stage (hazard ratio, 2.50; $P = 0.034$) were independent predictors (Table 3).

Validation in an independent cohort. The relative unresponsiveness of individuals with a high sIL6R level to PCRT was further validated in the independent cohort of 30 patients who received the same PCRT protocol (PCRT-validation Cohort). As the sIL6R level determined by a commercial ELISA kit was well correlated with that determined by the multiplexed immunobead-based assay ($R = 0.726$, Pearson's correlation coefficient) (Fig. S1), we used the kit for further measurements, since sandwich ELISA is generally accepted as a standard protocol for various clinical tests.

Among the PCRT-validation Cohort, 12% (4/34) of patients achieved a complete pathological response. There was no

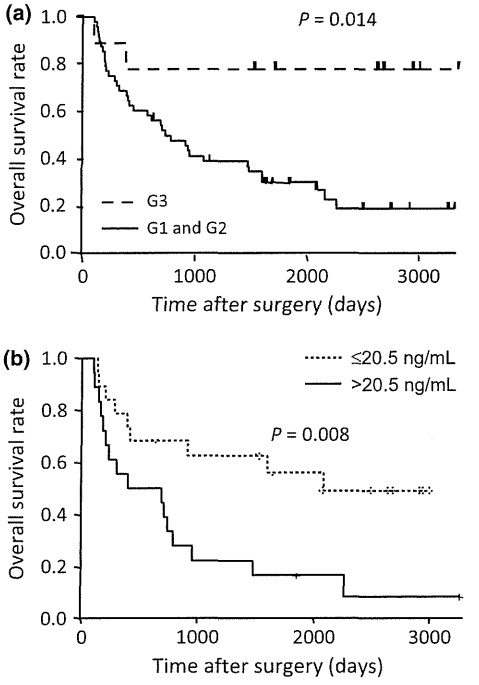


Fig. 1. Distinct outcomes of esophageal squamous cell carcinoma (ESCC) patients who achieved a pathological complete response to preoperative chemoradiotherapy (PCRT). (a) Kaplan–Meier estimates of overall postsurgical survival for seven ESCC patients of the PCRT-discovery Cohort who achieved a complete pathological response (G3) to PCRT and 30 patients who did not (G2 and G1). (b) Kaplan–Meier estimates of overall postsurgical survival for 18 ESCC patients of the PCRT-discovery Cohort having a baseline level of soluble interleukin-6 receptor higher than 20.5 ng/mL (median value of 37 patients), and for the remaining 19 patients.

Table 2. Six cytokines that differed significantly between esophageal squamous cell carcinoma patients whose histological response to preoperative chemoradiotherapy was graded G3, and those whose response was graded G1/2

Cytokines	G1 and G2 ($n = 30$)		G3 ($n = 7$)		*P*-value*
	Average (pg/mL)	SEM	Average (pg/mL)	SEM	
MIP1B	84.7	10.1	40.3	8.3	0.002
sIL6R	22528.6	1210.6	16520.7	1432.4	0.005
MIP1A	31.7	7.8	9.2	5.6	0.027
Insulin	2.1	0.6	0.6	0.0	0.031
IFNA2	386.1	172.6	25.7	25.5	0.048
MMP3	46396.2	5057.2	34817.6	2565.2	0.049

Histological responses graded according to the Japanese Classification of Esophageal Cancer (9th edition). **P*-values were calculated using Student's *t*-test. INFA2, interferon-α2; MIP1A, macrophage inflammatory protein α1; MIP1B, macrophage inflammatory protein 1-β; SEM, standard error of the mean; sIL6R, soluble interleukin-6 receptor.

© 2013 Japanese Cancer Association

Table 3. Cox regression model analysis of prognostic significance

Variable	Univariate analysis			Multivariate analysis		
	HR	95% CI	*P*-value	HR	95% CI	*P*-value
Age						
≥65 years/<65 years	1.31	0.57–2.96	0.521	–	–	–
Gender						
Male/female	0.31	0.07–1.33	0.115	–	–	–
Tumor location†						
Ce and Ut/Mt, Lt, and Ae	0.70	1.54–3.65	0.472	–	–	–
Clinical stage‡						
III and IVa/I and II	3.06	1.33–7.02	0.008	2.50	1.10–6.52	0.034
Serum sIL6R						
>20.5 ng/mL/≤20.5 ng/mL	3.20	1.34–7.53	0.008	2.87	1.20–6.85	0.017

†Tumor location was classified according to the Guidelines for Clinical and Pathologic Studies on Carcinoma of the Esophagus (9th edition).[17]
‡Clinical stage was classified according to the International Union Against Cancer's TNM Classification of Malignant Tumors (6th edition).[16]
Ae, abdominal esophagus; Ce, cervical esophagus; CI, confidence interval; HR, hazard ratio; Lt, lower thoracic esophagus; Mt, middle thoracic esophagus; sIL6R, soluble interleukin-6 receptor; Ut, upper thoracic esophagus.

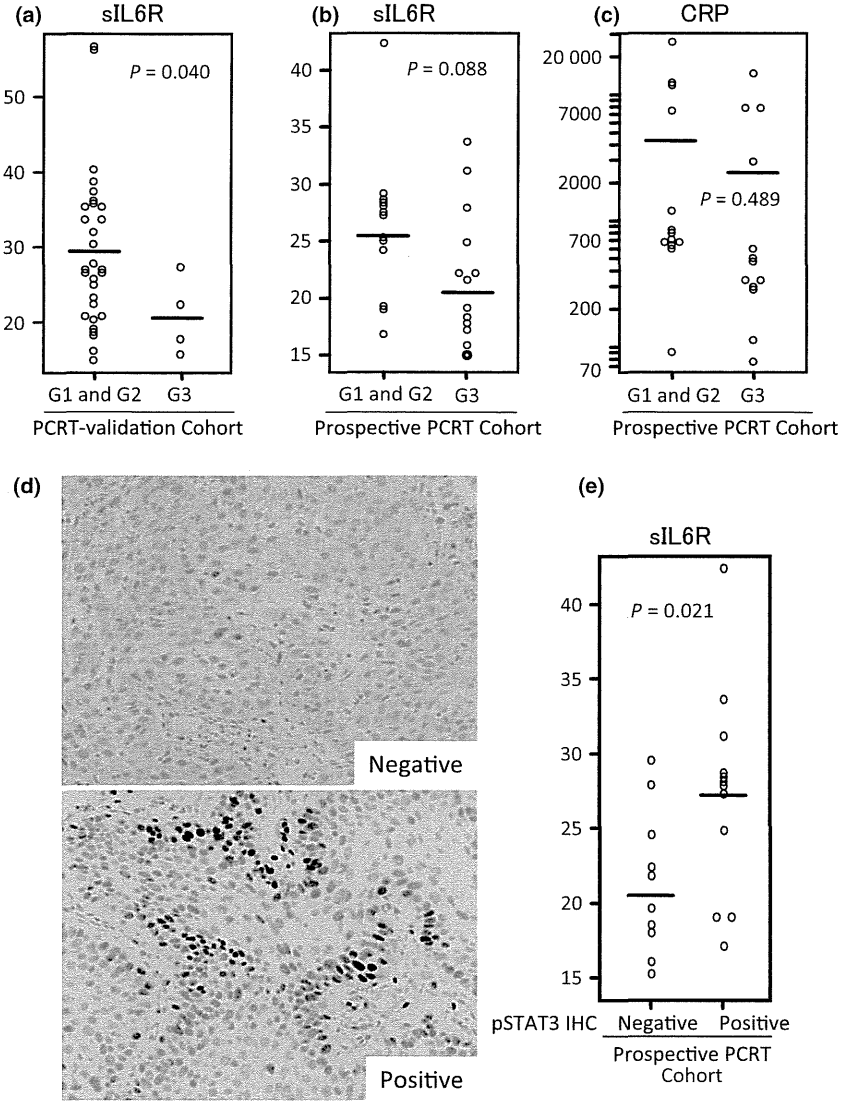


Fig. 2. Independent retrospective and prospective validation. (a) Soluble interleukin-6 receptor (sIL6R) level (ng/mL) in four esophageal squamous cell carcinoma (ESCC) patients who achieved a complete pathological response (G3) to preoperative chemoradiotherapy (PCRT) and 34 patients who did not (G1 and G2) in the PCRT-validation Cohort. Bars indicate mean values (G1 and G2, 29.6 ng/mL; G3, 21.4 ng/mL). (b) sIL6R levels (ng/mL) in 13 ESCC patients who achieved a complete pathological response (G3) to PCRT and 13 patients who did not (G1 and G2) in the prospective PCRT Cohort. Bars indicate mean values (G1 and G2, 25.2 ng/mL; G3, 21.7 ng/mL). (c) C-reactive protein (CRP) level (ng/mL) in 13 ESCC patients who achieved a complete pathological response (G3) to PCRT and 13 patients who did not (G1 and G2) in the prospective PCRT Cohort. Bars indicate mean values (G1 and G2, 4525.9 ng/mL; G3, 2859.7 ng/mL). (d) Representative phosphorylated signal transducer and activator of transcription-3 (pSTAT3)-negative (upper) and -positive (lower) cases. (e) sIL6R level (ng/mL) in 12 patients with ESCC positive for pSTAT3 and 10 patients with ESCC negative for pSTAT3. IHC, immunohistochemistry.

statistically significant difference in age, gender, tumor location, or clinical stage (Table 1), but the sIL6R level in the 4 patients who achieved a G3 response was significantly lower than in the remaining 34 patients ($P = 0.040$, *t*-test) (Fig. 2a).

Validation in a prospective cohort. We have recently completed a phase II clinical trial in which the efficacy of a new protocol for neoadjuvant chemoradiotherapy for clinical stage II–III ESCC was evaluated.[19] As a collateral study, we

doi: 10.1111/cas.12187
© 2013 Japanese Cancer Association

prospectively collected serum samples from patients participating in the trial (Prospective PCRT Cohort) and measured their levels of sIL6R and CRP.

Owing to the relatively intense PCRT protocol adopted in this clinical trial, 50% (13/26) of the patients achieved a G3 response. The level of sIL6R in those patients was lower than that in the remaining 13 who did not achieve a complete pathological response, with marginal statistical significance ($P = 0.088$) (Fig. 2b), but the CRP level did not show such a correlation ($P = 0.489$) (Fig. 2c).

To reveal the status of STAT3 signaling in patients with a high serum sIL6R level, the pretreatment tumor biopsy specimens from patients of the Prospective PCRT Cohort were immunostained with anti-pSTAT3 antibody. Intense nuclear staining of pSTAT3 in more than 30% of the tumor area was evident in 50% (13/26) of the cases, and these were classified as positive (Fig. 2d). The level of sIL6R was found to be significantly higher in pSTAT immunohistochemistry-positive cases than in negative cases ($P = 0.021$, t-test) (Fig. 2e).

Soluble interleukin-6 receptor is not a significant predictor of response to chemotherapy alone. Finally, we evaluated the sIL6R level in pretreatment serum samples from patients who received neoadjuvant combinational chemotherapy with CDDP /5-FU (PCT Cohort, $n = 100$) and docetaxel/CDDP/5-FU (prospective PCT Cohort, $n = 21$), and found that 7% (7/100) of patients in the PCT Cohort and 19% (4/21) of patients in the prospective PCT Cohort achieved a complete pathological G3 response.

There was no significant difference in sIL6R level between the seven individuals in the PCT Cohort who achieved a complete pathological response and the 93 individuals who did not ($P = 0.345$, t-test) (Fig. 3a), or between the four individuals in the PCT Cohort who achieved a complete pathological response and the 17 individuals who did not (Fig. 3b) ($P = 0.915$), indicating that sIL6R is a biomarker that predicts response to chemoradiotherapy, but not to chemotherapy. Consistently, the serum level of sIL6R had no significant correlation with the OS of patients in the PCT Cohort (Fig. 3c) ($P = 0.865$, log–rank test). These findings suggested that the pathways of tumor cell killing in response to chemotherapy and radiotherapy might differ.

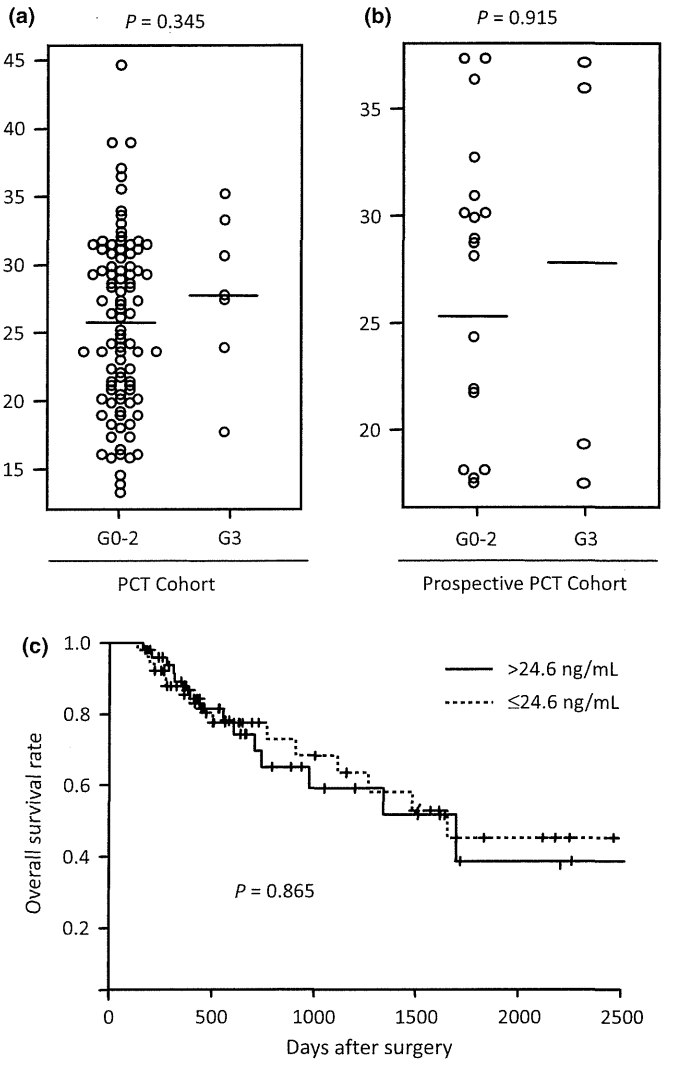


Fig. 3. Soluble interleukin-6 receptor (sIL6R) is not a significant predictor of response to chemotherapy alone. (a) sIL6R levels in seven esophageal squamous cell carcinoma (ESCC) patients who achieved a complete pathological response (G3) to preoperative chemotherapy (PCT) and 93 patients who did not (G0–2) in the PCT Cohort. Bars indicate mean values (G0–2, 25.6 pg/mL; G3, 27.9 pg/mL). (b) sIL6R level in 4 ESCC patients who achieved a complete pathological response (G3) to preoperative chemotherapy and 18 patients who did not (G0–2) in the prospective PCT Cohort. Bars indicate mean values (G0–2, 26.9 pg/mL; G3, 28.4 pg/mL). (c) Kaplan–Meier estimates of overall postsurgical survival of 49 ESCC patients with a serum level of sIL6R higher than 24.6 ng/mL (mean value of 100 patients) and the remaining 51 patients in the PCT Cohort.

Discussion

In the present study we showed for the first time that an increased serum level of sIL6R was correlated with a relatively poor response to PCRT in patients with ESCC. Several reports have documented the prognostic significance of serum CRP and IL6, but no biomarker that can predict the efficacy of PCRT for ESCC has yet been found.[24,25] The absence of any significant correlation with OS or pathological complete response in patients receiving chemotherapy alone (Fig. 3) indicated that sIL6R is not a prognostic biomarker. Squamous cell carcinoma is the predominant histological type of esophageal cancer in Asian countries[26] and accounts for >90% of surgical cases in Japan. It is generally accepted that the effects of PCRT are more apparent among patients with squamous cell carcinoma than in those with adenocarcinoma.[7,11]

Interleukin-6 receptor (also known as CD126) is a cell membrane cognate receptor for the inflammatory cytokine IL6.[27] Soluble IL6R is the alternatively spliced or proteolytically cleaved form of IL6R that lacks the transmembrane domain. Secreted sIL6R binds to IL6, and the sIL6R/IL6 complex evokes intracellular trans-signaling through binding to the gp130 receptor (CD130) expressed on the surface of various cells.[28] Soluble gp130, or sgp130, a soluble form of gp130,[29] competes with gp130 for binding to sIL6R/IL6. We measured the serum levels of IL6 and sgp130 in the PCRT-discovery Cohort, but found that they were not significantly correlated with response to PCRT (data not shown). A high level of sIL6R has been reported in patients with several chronic inflammatory and autoimmune diseases, as well as various malignancies.[27] Secretion and expression of IL6 and IL6R have been reported in esophageal cancer cells,[30,31] but the source of the increased sIL6R production in patients with esophageal cancer remains undetermined.

Although we were unable to reproduce those previous results in the present study cohorts (Fig. 2c and data not shown), some reports have documented that serum CRP and VEGF are correlated with the sensitivity of ESCC to PCRT.[31–33] C-reactive protein is produced by hepatocytes in response to inflammatory cytokines, such as IL6. The production of VEGF is

© 2013 Japanese Cancer Association

also regulated by IL6 signaling.[34] As well as sIL6R, we found that the levels of five cytokines (MIP1A, MIP1B, interferon-α2, insulin, and MMP3) were also significantly increased in patients who failed to achieve a complete pathological response (Table 2). Both MIP1A (also known as CCL3) and MIP1B (also known as CCL4) are cytokines released from macrophages in response to inflammatory stimuli. Alternatively, an increase in the levels of a variety of cytokines is considered to reflect a persistent systemic inflammatory status.

Suchi *et al.*[35] reported that overexpression of IL6 in ESCC cells induced resistance to cisplatin. The sIL6R/IL6 signal is transduced into the nucleus through JAK-mediated activation of STAT1/3.[27] Efimova *et al.*[36] reported that radiation-resistant human squamous cell carcinoma cells showed constitutive activation of the STAT1 pathway. Leu *et al.*[37] reported that IL6 inhibited apoptosis in human esophageal carcinoma cells through activation of the STAT3 and MAPK pathways. A small-molecule inhibitor of JAK2 (TG101209) has been reported to affect the expression of survivin, thus sensitizing lung cancer cells to radiation.[38] Here we observed that the nuclear expression of pSTAT3 was correlated with an increased level of circulating sIL6R (Fig. 2e). Based on these experimental and clinical findings, it would appear that active sIL6R/IL6/JAK/STAT signaling may be involved in the resistance of ESCC to PCRT.

However, there were certain limitations to this study in the context of potential clinical application. We observed that a substantial proportion of patients with a low level of sIL6R did not achieve a G3 response. Although patients with a high level of sILR6 may be potentially excluded from PCRT, we were unable to determine a safe cut-off value, mainly because of the small number of cases examined and the differences in therapy protocols among the cohorts. A substantially high proportion of patients in the Prospective PCRT Cohort achieved a complete response, and this included some patients with a high sIL6R level; this outcome was probably attributable to the intense nature of the therapy protocol. It will be necessary to carry out a large prospective study to evaluate the clinical applicability of our present findings. We are now planning a phase III clinical trial to compare the efficacies of preoperative combinational chemotherapy and chemoradiotherapy for ESCC.

Acknowledgments

This work was supported by a Grant-in Aid for Scientific Research from the Ministry of Education, Culture, Sports, Science and Technology of Japan, the National Cancer Center Research and Development Fund (23-A-38, and 23-A-11), and the Program for Promotion of Fundamental Studies in Health Sciences conducted by the National Institute of Biomedical Innovation of Japan. We thank Drs H. Fujiwara (Kyoto Prefectural University of Medicine, Kyoto, Japan) and S. Kikuchi (Hyogo College of Medicine, Nishinomiya, Japan) for helpful discussions.

Disclosure Statement

The authors have no conflict of interest.

Abbreviations

5-FU	5-fluorouracil
CDDP	cis-diamminedichloro-platinum (II) (cisplatin)
CRP	c-reactive protein
ESCC	esophageal squamous cell carcinoma
G0, G1, G2, G3	grades 0, 1, 2, 3
IL6	interleukin-6
MIP1A	macrophage inflammatory protein α1
MIP1B	macrophage inflammatory protein β1
NCC	National Cancer Center
OS	overall survival
PCRT	preoperative chemoradiotherapy
PCT	preoperative chemotherapy
pSTAT3	phosphorylated STAT3
(s)gp130	(soluble)gp130
sIL6R	soluble interleukin-6 receptor
STAT(1/3)	signal transducer and activator of transcription(-1/-3)
TMU	Tokyo Medical University
VEGF	vascular endothelial growth factor

References

1 Parkin DM, Bray FI, Devesa SS. Cancer burden in the year 2000. The global picture. *Eur J Cancer* 2001; **37**(Suppl. 8): S4–66.
2 Fiorica F, Di Bona D, Schepis F *et al.* Preoperative chemoradiotherapy for oesophageal cancer: a systematic review and meta-analysis. *Gut* 2004; **53**: 925–30.
3 Osaka Y, Takagi Y, Tsuchida A *et al.* Concurrent preoperative chemoradiotherapy for stage III or IV esophageal squamous carcinoma. *Oncol Rep* 2004; **12**: 1121–6.
4 Lee JL, Park SI, Kim SB *et al.* A single institutional phase III trial of preoperative chemotherapy with hyperfractionation radiotherapy plus surgery versus surgery alone for resectable esophageal squamous cell carcinoma. *Ann Oncol* 2004; **15**: 947–54.
5 Burmeister BH, Smithers BM, Gebski V *et al.* Surgery alone versus chemoradiotherapy followed by surgery for resectable cancer of the oesophagus: a randomised controlled phase III trial. *Lancet Oncol* 2005; **6**: 659–68.
6 Tepper J, Krasna MJ, Niedzwiecki D *et al.* Phase III trial of trimodality therapy with cisplatin, fluorouracil, radiotherapy, and surgery compared with surgery alone for esophageal cancer: CALGB 9781. *J Clin Oncol* 2008; **26**: 1086–92.
7 van Hagen P, Hulshof MC, van Lanschot JJ *et al.* Preoperative chemoradiotherapy for esophageal or junctional cancer. *N Engl J Med* 2012; **366**: 2074–84.
8 Berger AC, Farma J, Scott WJ *et al.* Complete response to neoadjuvant chemoradiotherapy in esophageal carcinoma is associated with significantly improved survival. *J Clin Oncol* 2005; **23**: 4330–7.
9 Kim MK, Kim SB, Ahn JH *et al.* Treatment outcome and recursive partitioning analysis-based prognostic factors in patients with esophageal squamous cell carcinoma receiving preoperative chemoradiotherapy. *Int J Radiat Oncol Biol Phys* 2008; **71**: 725–34.
10 Donahue JM, Nichols FC, Li Z *et al.* Complete pathologic response after neoadjuvant chemoradiotherapy for esophageal cancer is associated with enhanced survival. *Ann Thorac Surg* 2009; **87**: 392–8; discussion 8–9.
11 Kleinberg L, Forastiere AA. Chemoradiation in the management of esophageal cancer. *J Clin Oncol* 2007; **25**: 4110–7.
12 Geh JI. The use of chemoradiotherapy in oesophageal cancer. *Eur J Cancer* 2002; **38**: 300–13.
13 Budhu A, Forgues M, Ye QH *et al.* Prediction of venous metastases, recurrence, and prognosis in hepatocellular carcinoma based on a unique immune response signature of the liver microenvironment. *Cancer Cell* 2006; **10**: 99–111.
14 Seike M, Yanaihara N, Bowman ED *et al.* Use of a cytokine gene expression signature in lung adenocarcinoma and the surrounding tissue as a prognostic classifier. *J Natl Cancer Inst* 2007; **99**: 1257–69.
15 Suzuki Y, Mimura K, Yoshimoto Y *et al.* Immunogenic tumor cell death induced by chemoradiotherapy in patients with esophageal squamous cell carcinoma. *Cancer Res* 2012; **72**: 3967–76.
16 Sobin LH. *TNM Classification of Malignant Tumours*, 6th edn. New York: Wiley-Liss, 2002; 99–103.
17 The Japanese Society for Esophageal Disease. *Guidlines for the Clinical and Pathologic Studies on Carcinoma of the Esophagus*, 9th edn. In: Isono K, ed. Tokyo: Kanehara Shuppan, 2001.
18 Kikuchi S, Honda K, Tsuda H *et al.* Expression and gene amplification of actinin-4 in invasive ductal carcinoma of the pancreas. *Clin Cancer Res* 2008; **14**: 5348–56.
19 Kojima T, Hashimoto J, Kato K *et al.* Feasibility study of neoadjuvant chemoradiotherapy with cisplatin plus 5-fluorouracil and elective nodal

doi: 10.1111/cas.12187
© 2013 Japanese Cancer Association

irradiation for stage II/III esophageal squamous cell carcinoma. *J Clin Oncol* 2012; **37**(Suppl. 4): Abstract 130.
20 Honda K, Yamada T, Endo R *et al.* Actinin-4, a novel actin-bundling protein associated with cell motility and cancer invasion. *J Cell Biol* 1998; **140**: 1383–93.
21 Honda K, Yamada T, Hayashida Y *et al.* Actinin-4 increases cell motility and promotes lymph node metastasis of colorectal cancer. *Gastroenterology* 2005; **128**: 51–62.
22 Honda K, Hayashida Y, Umaki T *et al.* Possible detection of pancreatic cancer by plasma protein profiling. *Cancer Res* 2005; **65**: 10613–22.
23 Aickin M, Gensler H. Adjusting for multiple testing when reporting research results: the Bonferroni *vs* Holm methods. *Am J Public Health* 1996; **86**: 726–8.
24 Zingg U, Forberger J, Rajcic B, Langton C, Jamieson GG. Association of C-reactive protein levels and long-term survival after neoadjuvant therapy and esophagectomy for esophageal cancer. *J Gastrointest Surg* 2010; **14**: 462–9.
25 Shimada H, Nabeya Y, Okazumi S *et al.* Elevation of preoperative serum C-reactive protein level is related to poor prognosis in esophageal squamous cell carcinoma. *J Surg Oncol* 2003; **83**: 248–52.
26 Yamaji T, Inoue M, Sasazuki S *et al.* Fruit and vegetable consumption and squamous cell carcinoma of the esophagus in Japan: the JPHC study. *Int J Cancer* 2008; **123**: 1935–40.
27 Jones SA, Horiuchi S, Topley N, Yamamoto N, Fuller GM. The soluble interleukin 6 receptor: mechanisms of production and implications in disease. *FASEB J* 2001; **15**: 43–58.
28 Jones SA, Scheller J, Rose-John S. Therapeutic strategies for the clinical blockade of IL-6/gp130 signaling. *J Clin Invest* 2011; **121**: 3375–83.
29 Garbers C, Thaiss W, Jones GW *et al.* Inhibition of classic signaling is a novel function of soluble glycoprotein 130 (sgp130), which is controlled by the ratio of interleukin 6 and soluble interleukin 6 receptor. *J Biol Chem* 2011; **286**: 42959–70.
30 Oka M, Iizuka N, Yamamoto K *et al.* The influence of interleukin-6 on the growth of human esophageal cancer cell lines. *J Interferon Cytokine Res* 1996; **16**: 1001–6.
31 Fujiwara H, Suchi K, Okamura S *et al.* Elevated serum CRP levels after induction chemoradiotherapy reflect poor treatment response in association with IL-6 in serum and local tumor site in patients with advanced esophageal cancer. *J Surg Oncol* 2011; **103**: 62–8.
32 Shimada H, Takeda A, Nabeya Y *et al.* Clinical significance of serum vascular endothelial growth factor in esophageal squamous cell carcinoma. *Cancer* 2001; **92**: 663–9.
33 Shimada H, Kitabayashi H, Nabeya Y *et al.* Treatment response and prognosis of patients after recurrence of esophageal cancer. *Surgery* 2003; **133**: 24–31.
34 Jee SH, Shen SC, Chiu HC, Tsai WL, Kuo ML. Overexpression of interleukin-6 in human basal cell carcinoma cell lines increases anti-apoptotic activity and tumorigenic potency. *Oncogene* 2001; **20**: 198–208.
35 Suchi K, Fujiwara H, Okamura S *et al.* Overexpression of Interleukin-6 suppresses cisplatin-induced cytotoxicity in esophageal squamous cell carcinoma cells. *Anticancer Res* 2011; **31**: 67–75.
36 Efimova EV, Liang H, Pitroda SP *et al.* Radioresistance of Stat1 overexpressing tumour cells is associated with suppressed apoptotic response to cytotoxic agents and increased IL6-IL8 signalling. *Int J Radiat Biol* 2009; **85**: 421–31.
37 Leu CM, Wong FH, Chang C, Huang SF, Hu CP. Interleukin-6 acts as an antiapoptotic factor in human esophageal carcinoma cells through the activation of both STAT3 and mitogen-activated protein kinase pathways. *Oncogene* 2003; **22**: 7809–18.
38 Sun Y, Moretti L, Giacalone NJ *et al.* Inhibition of JAK2 signaling by TG101209 enhances radiotherapy in lung cancer models. *J Thorac Oncol* 2011; **6**: 699–706.

Supporting Information

Additional Supporting Information may be found in the online version of this article:

Fig. S1. Comparison of the multiplex bead-based assay and ELISA. The soluble interleukin-6 receptor level of 37 patients in the preoperative chemoradiotherapy (PCRT)-discovery Cohort was determined by the multiplex bead-based assay (*x*-axis) and ELISA (*y*-axis).

Table S1. Pathological criteria for evaluation of therapeutic efficacy.

Table S2. List of 84 cytokines and related proteins analyzed by the multiplexed immunobead-based assay.

Table S3. Correlation coefficients for six cytokines.

© 2013 Japanese Cancer Association

THE JOURNAL OF BIOLOGICAL CHEMISTRY VOL. 288, NO. 40, pp. 28488–28502, October 4, 2013
© 2013 by The American Society for Biochemistry and Molecular Biology, Inc. Published in the U.S.A.

F-box and WD Repeat Domain-containing-7 (Fbxw7) Protein Targets Endoplasmic Reticulum-anchored Osteogenic and Chondrogenic Transcriptional Factors for Degradation*[S]

Received for publication, February 26, 2013, and in revised form, August 15, 2013 Published, JBC Papers in Press, August 16, 2013, DOI 10.1074/jbc.M113.465179

Kanae Yumimoto[‡§], Masaki Matsumoto[‡§], Ichiro Onoyama[‡§], Kazunori Imaizumi[¶], and Keiichi I. Nakayama[‡§1]

From the [‡]Department of Molecular and Cellular Biology, Medical Institute of Bioregulation, Kyushu University, 3-1-1 Maidashi, Higashi-ku, Fukuoka, Fukuoka 812-8582, Japan, the [§]Core Research for Evolutional Science and Technology (CREST), Japan Science and Technology Agency (JST), Kawaguchi, Saitama 332-0012, Japan, and the [¶]Department of Biochemistry, Institute of Biomedical and Health Sciences, University of Hiroshima, 1-2-3 Kasumi, Minami-ku, Hiroshima 734-8553, Japan

Background: Fbxw7 is the F-box protein component of an SCF-type ubiquitin ligase that plays key roles in tumor suppression and stem cell maintenance.
Results: The transcription factors OASIS and BBF2H7 were identified as new substrates of Fbxw7.
Conclusion: Fbxw7 controls osteogenesis and chondrogenesis by targeting OASIS and BBF2H7 for degradation.
Significance: Fbxw7 is an important regulator of osteogenesis and chondrogenesis.

Although identification of substrates for an enzyme is a key step in elucidation of its biological functions, detection of the interaction between enzymes and substrates remains challenging. We recently developed a new approach, termed differential proteomics-based identification of ubiquitylation substrates (DiPIUS), for the discovery of substrates of ubiquitin ligases. We have now applied this approach to Fbxw7, the F-box protein component of an Skp1-Cul1-F-box protein-type ubiquitin ligase and, thereby, identified two similar transcription factors, old astrocyte specifically induced substance (OASIS) and BBF2 human homolog on chromosome 7 (BBF2H7), as candidate substrates. Coimmunoprecipitation analysis confirmed that the α and γ isoforms of Fbxw7 interact with OASIS and BBF2H7 *in vivo*. Sustained overexpression of Fbxw7 resulted in marked down-regulation of OASIS and BBF2H7, whereas RNAi-mediated Fbxw7 depletion stabilized both proteins. Mutation of a putative Cdc4 phosphodegron in OASIS and BBF2H7 attenuated their association with Fbxw7 and resulted in their stabilization. Depletion of Fbxw7 promoted the differentiation of mouse C2C12 mesenchymal cells into osteoblasts in association with the accumulation of OASIS. Conversely, overexpression of Fbxw7 in C2C12 cells resulted in down-regulation of Col1A1 mRNA, a target of OASIS. Conditional ablation of *Fbxw7* in primary mouse mesenchymal cells promoted chondrogenesis in association with up-regulation of BBF2H7, whereas overexpression of Fbxw7 inhibited chondrogenesis in ATDC5 cells. Collectively, our results suggest that OASIS and BBF2H7 are *bona fide* substrates of Fbxw7 and that Fbxw7 controls osteogenesis and chondrogenesis by targeting OASIS and BBF2H7, respectively, for degradation.

The Skp1-Cul1-F-box protein (SCF)[2] complex is one of the most well characterized types of ubiquitin ligase. Each SCF complex consists of four subunits: Skp1, Cul1, Rbx1 (also known as Roc1 or Hrt1), and an F-box protein (1–3). F-box proteins are responsible for substrate recognition by each complex and constitute a large family of > 70 eukaryotic proteins (4). The F-box protein Fbxw7 was initially identified as a negative regulator of LIN-12 (Notch)-mediated signaling in *Caenorhabditis elegans* by genetic analysis (5, 6). It was shown subsequently to play a pivotal role in the control of cell proliferation through ubiquitylation of cyclin E (7–9), c-Myc (10, 11), Notch (5, 12, 13), c-Jun (14, 15), and Krüppel-like factor (KLF) 5 (16, 17). Given its function in the degradation of proliferation-related proteins, Fbxw7 is thought to act as a tumor suppressor protein. Indeed, ~6% of primary human tumors have been found to harbor mutations in *FBXW7* (18), with the mutations being detected most frequently in cholangiocarcinoma (35%) and T cell acute lymphocytic leukemia (31%).

In addition to tumor suppression, Fbxw7 has been shown recently to contribute to stem cell maintenance and cell differentiation. Thus, it regulates the quiescence and self-renewal of hematopoietic stem cells and neural stem cells (19–23) as well as of leukemia stem cells (24–26). The loss of Fbxw7 in neural stem cells also impairs their differentiation into neurons as a result of the up-regulation of Notch (22, 23). Fbxw7 deficiency in intestinal crypts also leads to the accumulation of progenitor cells and impairment of their differentiation into goblet cells (27, 28). Conditional ablation of *Fbxw7* in the liver results both in a shift in the differentiation of liver stem cells from the he-

* This work was supported in part by a grant from the Ministry of Education, Culture, Sports, Science, and Technology of Japan.
[S] This article contains supplemental Table S1.
[1] To whom correspondence should be addressed: Dept. of Molecular and Cellular Biology, Medical Institute of Bioregulation, Kyushu University, 3-1-1 Maidashi, Higashi-ku, Fukuoka, Fukuoka 812-8582, Japan. Tel.: 81-92-642-6815; Fax: 81-92-642-6819; E-mail: nakayak1@bioreg.kyushu-u.ac.jp.

[2] The abbreviations used are: SCF, Skp1-Cul1-F-box protein; SREBP, sterol response element-binding protein; OASIS, old astrocyte specifically induced substance; BBF2H7, BBF2 human homolog on chromosome 7; ER, endoplasmic reticulum; DAPT, *N*-[*N*-(3,5-difluorophenacetyl)-L-alanyl]-*S*-phenylglycine *t*-butyl ester; DiPIUS, differential proteomics-based identification of ubiquitylation substrates; DiPIUS-NL, differential proteomics-based identification of ubiquitylation substrates nonlabeling; SILAC, stable isotope labeling with amino acids in cell culture; IPI, International Protein Index; CPD, Cdc4 phosphodegron; FL, full-length; N, nuclear.

Downloaded from http://www.jbc.org/ at FUZOKU TOSHOKAN KYUSHU UNIV on February 1, 2014

patocyte lineage to cholangiocytes as well as in increased cell proliferation (29). Liver-specific deficiency of Fbxw7 also results in lipid accumulation in hepatocytes as a consequence of the accumulation of its targets KLF5 and sterol response element-binding proteins (SREBPs) (29, 30). In cultured cells, Fbxw7 deficiency promotes the formation of lipid droplets as a result of the accumulation of SREBPs and CCAAT/enhancer-binding protein α (c/EBPα) (31, 32). Collectively, these observations indicate that Fbxw7 regulates various developmental and differentiation processes by targeting multiple substrate molecules for degradation.

OASIS (CREB3L1) and BBF2H7 (CREB3L2) are basic leucine zipper-type transcription factors that belong to the cAMP response element-binding protein (CREB)/activating transcription factor family. Both proteins possess a transmembrane domain that allows them to associate with the endoplasmic reticulum (ER) and is cleaved by site 1 and site 2 proteases (S1P and S2P) in response to ER stress (33, 34). Expression of OASIS is restricted to certain tissues and cells, including astrocytes and osteoblasts (35, 36). OASIS-deficient mice manifest severe osteopenia that is associated with a decrease in the amount of type I collagen in the bone matrix and a reduced activity of osteoblasts (37). Expression of OASIS in osteoblasts is induced by bone morphogenetic protein 2 (BMP2), signaling by which is required for bone formation, and OASIS up-regulates transcription of the gene for the type I collagen Col1A1 directly. BBF2H7 is highly expressed in the proliferating zone of cartilage in developing long bones (38). Mice deficient in BBF2H7 manifest pronounced chondrodysplasia and die from choking after birth as a result of immaturity of the chest cavity. Type II collagen (Col2) and cartilage oligomeric matrix protein accumulate in the ER lumen of BBF2H7-deficient chondrocytes. BBF2H7 directly activates transcription of the gene for Sec23a, a component of coat protein complex II responsible for protein transport from the ER to the Golgi apparatus, suggesting that BBF2H7 controls the secretion of extracellular matrix molecules in cartilage by regulating vesicle transport.

We now show that OASIS and BBF2H7 are targets of SCF^{Fbxw7}. Fbxw7 controls osteoblast and chondrocyte differentiation by targeting OASIS and BBF2H7 for proteasome-mediated degradation. Thus, our results suggest that Fbxw7 is an important regulator of osteogenesis and chondrogenesis.

EXPERIMENTAL PROCEDURES

Cell Culture—Neuro2A cells, mHepa cells, C2C12 cells, and HeLa cells stably expressing murine cationic amino acid transporter type 1 (mCAT-HeLa cells) were maintained in DMEM supplemented with 10% FBS (Invitrogen), 1 mM sodium pyruvate, penicillin (100 units/ml, Invitrogen), streptomycin (100 mg/ml, Invitrogen), 2 mM L-glutamine, and nonessential amino acids (10 ml/l, Invitrogen). Differentiation of C2C12 cells toward the osteoblast lineage was induced by their exposure for 6 days to recombinant human BMP2 (300 ng/ml, Shenandoah Biotechnology) in DMEM supplemented with 2.5% FBS. The differentiated cells were washed with PBS, fixed in Bouin's solution for 1 h, washed with distilled H_2O, stained with 0.1% Sirius red (Direct Red 80, Sigma) for 1 h at 37 °C, and then washed with 10 mM HCl. The murine chondrogenic cell line ATDC5 was cultured in a 1:1 (v/v) mixture of DMEM and Ham's F12 medium (Invitrogen) that was supplemented with 5% FBS, human transferrin (10 μg/ml, Sigma), 30 nM sodium selenite (Sigma), 1 mM sodium pyruvate, penicillin (100 units/ml), streptomycin (100 mg/ml), 2 mM L-glutamine, and nonessential amino acids (10 ml/l). For induction of chondrogenesis, ATDC5 cells were plated at an initial density of 6250 cells/cm^2 and cultured for 16 days in medium supplemented with bovine insulin (10 μg/ml, Sigma). For inhibition of Notch signaling, the cells were also cultured with the γ-secretase inhibitor *N*-[*N*-(3,5-difluorophenacetyl)-L-alanyl]-*S*-phenylglycine *t*-butyl ester (DAPT, Calbiochem). For Alcian blue staining, the cells were washed twice with PBS, fixed in 3.7% formaldehyde for 10 min, and stained overnight with 0.1% Alcian blue in 0.1 M HCl. The cells were then solubilized with 6 M guanidine hydrochloride for measurement of A_{595} with a spectrophotometer. Sf21 cells were cultured at 27 °C in Sf-900 II SFM medium (Invitrogen) supplemented with 5% FBS (Invitrogen), penicillin (100 units/ml, Invitrogen), and streptomycin (100 mg/ml, Invitrogen).

Antibodies—Antibodies to KLF5 (BTEB2, H-300) and to c-Myc (N-262) were obtained from Santa Cruz Biotechnology. Antibodies to Skp1 and to Hsp90 were from BD Biosciences. Antibodies to 14-3-3ϵ were from BD Transduction Laboratories. Antibodies to Cul1 were from Zymed Laboratories Inc.. Antibodies to the HA epitope (HA11) were from Babco. Antibodies to the FLAG epitope (M2) were from Sigma. Antibodies to GAPDH (1D4) were from Assay Designs. Antibodies to protein disulfide isomerase were from Thermo Scientific. Antibodies to cleaved Notch1 (Val^{1744}) were from Cell Signaling Technology. Antibodies to OASIS and BBF2H7 were described previously (37, 38).

Plasmids—Complementary DNAs encoding mouse Fbxw7α or its ΔF mutant were subcloned into p3×FLAG-CMV 7.1 (Sigma), and those for HA epitope- or FLAG epitope-tagged human OASIS or BBF2H7 were subcloned into pcDNA3 (Invitrogen). The resulting vectors were introduced into mCAT-HeLa cells with the use of the FuGENE 6 or FuGENE HD transfection reagents (Roche or Promega). For retroviral expression, cDNAs for FLAG-tagged mouse Fbxw7α, Fbxw7β, Fbxw7γ, or corresponding mutants or those for HA epitope-tagged human OASIS, BBF2H7, or corresponding mutants were subcloned into pMX-puro (provided by T. Kitamura). The resulting vectors were introduced into Plat E cells with the use of FuGENE HD. The recombinant retroviruses generated thereby were used to infect mCAT-HeLa or HEK293T cells, which were then subjected to selection in medium containing puromycin (10 μg/ml). For baculoviral expression, cDNAs for FLAG-tagged mouse Fbxw7α, Myc epitope-tagged mouse Cul1 and Skp1, and HA epitope-tagged NH_2-terminal fragments of human OASIS and BBF2H7 were subcloned into pFASTBacHT (encoding a His_6 tag), whereas that for human Rbx1 containing an NH_2-terminal Myc epitope tag was subcloned into pFASTBac1.

DiPIUS and DiPIUS-NL—DiPIUS and DiPIUS-NL were performed as described (39). For DiPIUS on the basis of stable isotope labeling with amino acids in cell culture (SILAC), WT and ΔF mutant forms of Fbxw7α with an NH_2-terminal FLAG tag were expressed in light isotope- and heavy isotope-labeled

mCAT-HeLa cells, respectively. The cells (2×10^7) were incubated for 6 h in the presence of the proteasome inhibitor MG132 (10 μM, Peptide Institute) and were then lysed in 8 ml of a solution containing 20 mM HEPES-NaOH (pH 7.5), 150 mM NaCl, 1% digitonin, 10 mM NaF, 10 mM $Na_4P_2O_7$, 0.4 mM Na_3VO_4, 0.4 mM EDTA, 20 μg/ml leupeptin, 10 μg/ml aprotinin, and 1 mM PMSF. The lysates were centrifuged at 2200 × *g* for 20 min at 4 °C to remove debris, and the resulting supernatants were adjusted with lysis buffer to a protein concentration of 2.5 mg/ml. The supernatants (20 mg of protein in 8 ml of solution) from light-labeled cells and heavy-labeled cells were then combined and incubated for 1 h at 4 °C with 120 μl of beads conjugated with M2 antibodies to FLAG (Sigma). The beads were washed three times with 4 ml of a solution containing 10 mM HEPES-NaOH (pH 7.5), 150 mM NaCl, and 0.1% Triton X-100, and bead-bound proteins were then eluted with the FLAG peptide (500 μg/ml, Sigma), precipitated with ice-cold 20% trichloroacetic acid, and washed with acetone.

The concentrated proteins were digested with Lys-C and trypsin, and the resulting peptides were analyzed with an LTQ Orbitrap Velos LC-MS/MS system (Thermo Finnigan). The peak lists were generated with Mascot Distiller (version 2.3.0) and were compared with the "Target-decoy" Human IPI database (version 3.1.6, see below) with the use of the MASCOT algorithm (version 2.2.1). Trypsin was selected as the protease, the allowed number of missed cleavages was set to one, and carbamidomethylation of cysteine was selected as the fixed modification. Oxidized methionine, pyroglutamine, $^{13}C_6$-lysine, and $^{13}C_6$-arginine were searched as variable modifications. Precursor mass tolerance was 20 ppm, and tolerance of MS/MS ions was 0.8 Da. Assigned high-scoring peptide sequences (MASCOT score > 20) were processed with in-house software. If the MASCOT score was < 45, assigned sequences were confirmed manually as described below for spectral counting, and the false discovery rate at the peptide level was estimated. SILAC quantitation was performed with the use of the Mascot Distiller Quantitation Tool (version 2.3.0). Extracted ion chromatogram peak areas for the heavy and light peptides were measured, and the results were verified by manual inspection of MS spectra. SILAC ratios were calculated by comparison of the extracted ion chromatogram peak areas of light peptides with those of the heavy peptides. The method "Auto" was selected for the removal of outlier peptide pairs (peptides with a number between 4 and 25 by Dixon's method or of > 25 by Rosner's method). SILAC ratios for different peptides of a protein were averaged to give protein abundance ratios, which were then normalized with the heavy/light ratio for Fbxw7α.

For DiPIUS-NL on the basis of spectral counting, the concentrated immunoaffinity-purified proteins derived separately from lysates of nonlabeled cells expressing FLAG-tagged WT or ΔF mutant forms of Fbxw7α were dissolved in SDS sample buffer, fractionated by SDS-PAGE, and stained with silver. Individual lanes of the stained gel were sliced into 8 to 16 pieces, and proteins within these pieces were subjected to in-gel digestion with trypsin as described previously (40). The resulting peptides were dried and then dissolved in a solution containing 0.1% trifluoroacetic acid and 2% acetonitrile before analysis with an ion-trap mass spectrometer (LTQ-XL, Thermo Finnigan). Peak lists were generated with lcq_dta.exe (Thermo Finnigan) and compared with the use of the MASCOT algorithm (version 2.2.1) either with the "Target-decoy" Human IPI database (version 3.1.6, released in November 2006, with 62,322 target sequences, searched against a total of 124,644 sequences (target and reverse/decoy)) or with the "Target-decoy" Mouse IPI database (version 3.4.4, released in June 2008, with 55,078 target sequences, searched against a total of 110,156 sequences (target and reverse/decoy)), both maintained by the European Bioinformatics Institute. Trypsin was selected as the protease, the allowed number of missed cleavages was set to one, and carbamidomethylation of cysteine was selected as the fixed modification. Oxidized methionine and pyroglutamine were searched as variable modifications. Precursor mass tolerance was 1.5 Da, and tolerance of MS/MS ions was 0.8 Da. Assigned high-scoring peptide sequences (MASCOT score > 35) were processed with in-house software. If the MASCOT score was < 45 (peptides for which the MS2 score was above the 95th percentile of significance), assigned sequences were manually confirmed by comparison with the corresponding collision-induced dissociation spectra on the basis of the following criteria: 1) a Δ score of > 15 or 2) at least six successive matches for y- or b-ions or at least three blocks of three successive matches for y- or b-ions. Identified peptides from independent experiments were integrated and regrouped by IPI accession number. When multiple accession numbers were obtained with the same set of peptides, a representative IPI accession was chosen according to the following order of priorities: 1) IPI accession containing NCBI GeneID, 2) IPI accession with the use of Swiss-Prot as the master sequence, and 3) IPI accession with the use of Translated European Molecular Biology Laboratory (TrEMBL) as the master sequence. Proteins identified in only one experiment or with a single-peptide assignment were removed from spectral counting data. Estimated false discovery rates were zero at the protein level.

RNAi—Construction of shRNA vectors and RNAi were performed as described previously (41). The sequences targeted for human or mouse Fbxw7 and mouse OASIS were 5′-GCAAATGTCTGAGAACATTAG-3′ (human Fbxw7 RNAi-1), 5′-GGTTGTTAGTGGAGCATATGA-3′ (human Fbxw7 RNAi-2), 5′-GGTTCTGAAGTTCGTTCCTTT-3′ (mouse Fbxw7), and 5′-GCATTCTCTTCCGGCTCAATG-3′ (mouse OASIS). An RNAi vector for enhanced GFP was used as a control.

RT and Real-time PCR Analysis—Total RNA (1 μg) isolated from cells with the use of Isogen (Nippon Gene) was subjected to RT with a QuantiTect reverse transcription kit (Qiagen), and the resulting cDNA was subjected to real-time PCR analysis with SYBR Green PCR Master Mix and specific primers in a StepOnePlus real-time PCR system (Applied Biosystems). The sequences of the various primers (sense and antisense, respectively) were 5′-TCTGAGGTCCGCTCTTTTTCTT-3′ and 5′-TGAGGTCCCCAAAAGTTGTTG-3′ for human Fbxw7; 5′-TGAAGTTCGTTCCTTTTCTTTGG-3′ and 5′-CAAAAGTTGTTGGTGTTGCTGAA-3′ for mouse Fbxw7; 5′-GCCTAAAGACGGTGGAAACG-3′ and 5′-GGCATGGACCTAGGAGGTTTG-3′ for human OASIS; 5′-CTGAGCACAGCTACTCCCTG-3′ and 5′-CCGTGTTCCACATCTTGAGT-3′ for

Downloaded from http://www.jbc.org/ at FUZOKU TOSHOKAN KYUSHU UNIV on February 1, 2014

mouse OASIS; 5′-AGAACTTGGAGCTTCGGAAGAA-3′ and 5′-GCTAACTTGCAGGTTCGAGAAAC-3′ for human BBF2H7; 5′-CTCATGCCAGACGCTTATTCC-3′ and 5′-ACTGGGTGGTGTTGGTGGTAA-3′ for mouse BBF2H7; 5′-TGGTCCTGCTACCCAGGGGC-3′ and 5′-TCTGGTCCAACGCACAGGCG-3′ for mouse Sec23a; 5′-CCCCAACCCTGGAAACAGAC-3′ and 5′-GGTCACGTTCAGTTGGTCAAAGG-3′ for mouse Col1A1; 5′-CAGGGCTGCTTTTAACTCTGGTA-3′ and 5′-GGGTGGAATCATATTGGAACATG-3′ for human GAPDH; and 5′-AGGTTGTCTCCTGCGACTTCA-3′ and 5′-CCAGGAAATGAGCTTGACAAAGTT-3′ for mouse GAPDH. The amounts of target mRNAs were normalized by that of GAPDH mRNA.

Immunoprecipitation, Cycloheximide Chase, and Immunoblot Analyses—Cells were incubated for 6 h in the presence of MG132 (10 μM) before lysis for immunoprecipitation. The cells were lysed by incubation for 20 min at 4 °C with a solution containing 50 mM Tris-HCl (pH 7.5), 150 mM NaCl, 0.5% Triton X-100, 10 mM NaF, 10 mM $Na_4P_2O_7$, 0.4 mM Na_3VO_4, 0.4 mM EDTA, leupeptin (20 μg/ml), and aprotinin (10 μg/ml). The lysates were centrifuged at 20,400 × *g* for 20 min at 4 °C, and equal amounts of protein from the resulting supernatants were subjected to immunoprecipitation for 1 h at 4 °C with anti-FLAG (M2)-agarose affinity gel (Sigma). For cycloheximide chase experiments, cycloheximide (50 μg/ml) was added to culture medium, and cells were harvested at the indicated times thereafter. Immunoprecipitates and cell lysates were subjected to immunoblot analysis as described (42), with Hsp90, GAPDH, and 14-3-3ε used as loading controls. For Phos-tag SDS-PAGE, a standard discontinuous 8% polyacrylamide gel was prepared with the modification that 10 μM Phos-tag reagent (Wako) and 40 μM $MnCl_2$ were added to the separation gel mix before polymerization. After electrophoresis, the gel was incubated for 40 min in Western transfer buffer containing 10 mM EDTA and for 10 min in transfer buffer.

Immunofluorescence Staining—mCAT-HeLa cells grown on glass coverslips were transfected with expression vectors with the use of the FuGENE HD reagent and subsequently prepared for immunostaining. The cells were fixed for 10 min at 37 °C with 4% paraformaldehyde in PBS and then incubated first overnight at 4 °C with primary antibodies in PBS containing 0.5% Triton X-100 and then for 1 h at room temperature with Alexa Fluor 488- or Alexa Fluor 546-labeled secondary antibodies (dilution of 1:2000, Molecular Probes). The cells were finally stained with Hoechst 33258 (Wako), covered with a drop of Fluoromount (Diagnostic BioSystems), and examined with a laser-scanning confocal microscope (LSM510, Carl Zeiss).

In Vitro Ubiquitylation Assays—Recombinant ubiquitin and purified rabbit Uba1 (E1) were obtained from Sigma and Lifesensors, respectively. Human UbcH5C (E2) was expressed in and purified from *Escherichia coli* as described (42). Recombinant baculoviruses were generated with the Bac-to-Bac (Invitrogen) baculovirus systems. Sf21 cells that had been infected with baculoviruses encoding Fbxw7α, Cul1, Skp1, and Rbx1 were lysed on ice with the lysis buffer used for immunoprecipitation, and the expressed proteins were purified with the use of beads conjugated with M2 antibodies to FLAG. The beads were washed three times with a solution containing 10 mM HEPES-NaOH (pH 7.5), 150 mM NaCl, and 0.1% Triton X-100, and the bead-bound proteins were then eluted with the FLAG peptide (500 μg/ml). Sf21 cells that had been infected with baculoviruses encoding His_6-tagged HA-OASIS(N) or HA-BBF2H7(N) were lysed on ice with a solution containing 50 mM Tris-HCl (pH 8.0), 500 mM NaCl, 10 mM imidazole, 1% Nonidet P-40, 20 μg/ml leupeptin, and 10 μg/ml aprotinin, and the recombinant proteins were purified by Ni^{2+}-agarose chromatography as described (43). To determine the ability of the purified recombinant $SCF^{Fbxw7\alpha}$ complex to mediate the ubiquitylation of OASIS(N) and BBF2H7(N), we incubated the complex (400 ng) for 2 h at 30 °C with 100 ng of Uba1, 500 ng of UbcH5C, 1 μg of ubiquitin, and 400 ng of either OASIS(N) or BBF2H7(N) in a final volume of 20 μl containing 25 mM Tris-HCl (pH 7.5), 120 mM NaCl, 2 mM ATP, 1 mM $MgCl_2$, 1 mM DTT, 0.5 units of phosphocreatine kinase, and 1 mM creatine phosphate. The reaction mixtures were then subjected to immunoblot analysis with antibodies to HA.

Identification of Phosphorylation Sites by LC-MS/MS Analysis—FLAG-tagged OASIS and BBF2H7 were expressed, purified, and concentrated as described above for FLAG-Fbxw7α in DiPIUS-NL. The protein preparations were fractionated by SDS-PAGE and stained with silver, and bands corresponding to the full-length forms of OASIS and BBF2H7 were excised and subjected to in-gel digestion with trypsin. The resulting peptides were dried, dissolved in a mixture of 0.1% trifluoroacetic acid and 2% acetonitrile, and then applied to a nanoflow LC system (Michrom BioResources) equipped with an L-column (C_{18}, 0.1 by 160 mm, particle size of 3 μm, CERI, Tokyo, Japan). The peptides were fractionated with a linear gradient of solvent A (0.1% formic acid in water) and solvent B (100% acetonitrile), with 5–45% solvent B over 40 min, 45–95% over 1 min, 95% over 2 min, and 95–5% over 2 min at a flow rate of 0.2 μl/min. They were then sprayed directly into a Q-Exactive mass spectrometer (Thermo Fisher). MS and MS/MS spectra (top 10 peaks) were obtained automatically in a data-dependent scan mode with a dynamic exclusion option. For protein identification, tandem mass spectra were extracted, and the charge state deconvoluted with Proteome Discoverer 1.3.0.339 (Thermo Fisher). All MS/MS spectra were compared with protein sequences in the IPI database (human version 3.26, released February 2007, 67,665 sequences, 28,353,548 residues) with the use of the MASCOT algorithm (version 2.3.02). An error of 10 ppm or 0.01 Da was set for full searches of MS and MS/MS spectra, respectively. Trypsin was selected as the enzyme used, the allowed number of missed cleavages was set at two, and carbamidomethylation of cysteine was selected as a static modification. Oxidized methionine, NH_2-terminal pyroglutamine, NH_2-terminal acetylation, and phosphorylation of Ser, Thr, or Tyr were specified as dynamic modifications. The ions score cutoff was 10. The phosphoRS mode of Proteome Discoverer was used for phosphorylation site localization.

Mice and Primary Culture of Chondrocytes—For generation of *CAG-CreERT2;Fbxw7*$^{F/F}$ mice, *CAG-CreERT2* mice (44) were crossed with *Fbxw7*$^{F/F}$ mice (45). For primary chondrocyte culture, mesenchymal cells were prepared from the limbs of mouse embryos at embryonic day 11.5 by digestion with 0.1% trypsin and 0.1% collagenase D. Cells were plated at a density of

2×10^7 cells/ml and maintained in α-minimum essential medium supplemented with 10% FBS, ascorbic acid (50 μg/ml), and β-glycerophosphate (5 mM). Tamoxifen (2 μM, Sigma) was added to the culture medium to induce expression of Cre recombinase, and the cells were analyzed at the indicated times thereafter.

Statistical Analysis—Data are presented as mean ± S.D. and were analyzed with the Tukey-Kramer multiple comparison test. $p < 0.05$ was considered statistically significant.

RESULTS

Isolation of Substrates for SCF^{Fbxw7} by DiPIUS—To comprehensively isolate the substrates for a given F-box protein, we developed a differential proteomics approach termed differential proteomics-based identification of ubiquitylation substrates (DiPIUS) (39). The DiPIUS system is on the basis of a difference in binding affinity for substrates between WT and mutant F-box proteins. Wild-type F-box proteins bind weakly to their substrates, which are then ubiquitylated and undergo subsequent degradation, whereas F-box proteins with a deletion in the F-box domain might be expected to associate stably with substrates and thereby allow them to accumulate in the cell (Fig. 1*A*).

Both WT Fbxw7α and a mutant form of the protein lacking the entire F-box domain (ΔF mutant) were tagged at their NH_2 termini with the FLAG epitope and expressed separately in HeLa cells. Cell lysates were subjected to immunoprecipitation with antibodies to FLAG, and the immunoprecipitated proteins were analyzed by LC-MS/MS. The abundance of proteins that bound to the WT or mutant F-box proteins was compared by quantitative SILAC analysis (original DiPIUS) or semiquantitative spectral counting (DiPIUS-NL) (Fig. 1*A*). We identified OASIS (CREB3L1) and BBF2H7 (CREB3L2) as candidate substrates of Fbxw7α with both the DiPIUS (Fig. 1, *B–D*) and DiPIUS-NL (Fig. 1*E*) systems in HeLa cells (39). OASIS was also detected as a candidate substrate in C2C12 cells, whereas BBF2H7 was so identified in mHepa, Neuro2A, and C2C12 cells. We also examined the interaction between Fbxw7α and endogenous OASIS or BBF2H7 in HeLa cells by coimmunoprecipitation analysis. We treated the cells with the proteasome inhibitor MG132 for 6 h before immunoprecipitation to prevent the degradation of OASIS and BBF2H7 and, thereby, maximize their interaction with Fbxw7α. Such an analysis verified that endogenous OASIS and BBF2H7 interacted with Fbxw7α(ΔF) more efficiently than with Fbxw7α(WT) in HeLa cells (Fig. 1, *F* and *G*).

OASIS and BBF2H7 Interact with Fbxw7α and Fbxw7γ but not with Fbxw7β—The full-length (FL) forms of OASIS and BBF2H7 are cleaved in response to ER stress, and the released NH_2-terminal cytoplasmic domain (N) of each protein activates the transcription of target genes. Fbxw7 exists in three isoforms (Fbxw7α, Fbxw7β, and Fbxw7γ) that differ in their NH_2-terminal regions and subcellular distributions. Fbxw7α is localized to the nucleus, Fbxw7β shows a cytoplasmic distribution suggestive of localization to the ER and Golgi apparatus, and Fbxw7γ is predominantly nucleolar (3), suggesting that each isoform might interact with a different set of substrates. We constructed vectors for versions of the three Fbxw7 isoforms with a 3× FLAG tag inserted on the NH_2-terminal side of the dimerization domain, designated FLAG(M)-Fbxw7α, FLAG(M)-Fbxw7β, and FLAG(M)-Fbxw7γ (Fig. 2*A*). To investigate the contribution of each isoform of Fbxw7 to the interaction with OASIS and BBF2H7, we performed coimmunoprecipitation experiments with the FLAG(M)-tagged Fbxw7 proteins expressed in HEK293T cells. Fbxw7α interacted efficiently with the N forms of both OASIS and BBF2H7 and, to a lesser extent, with the FL form of each protein (Fig. 2, *B* and *C*). Fbxw7γ interacted at a low level with both FL and N forms of OASIS and BBF2H7, but we did not detect any interaction between Fbxw7β and OASIS or BBF2H7. We speculate that the anchoring of Fbxw7β and the FL forms of OASIS and BBF2H7 to the ER membrane may structurally impede the interaction of these proteins.

We examined the subcellular localization of HA epitope-tagged OASIS and BBF2H7 by immunofluorescence analysis in cells incubated with or without MG132. In the absence of MG132 treatment, HA-OASIS and HA-BBF2H7 were colocalized with the ER marker protein disulfide isomerase, whereas MG132 promoted the cleavage of these proteins at the ER and stabilized the cleaved forms, resulting in the accumulation of HA-OASIS(N) and HA-BBF2H7(N) in the nucleus (Fig. 2*D*). We also examined the localization of FLAG(M)-tagged Fbxw7α, Fbxw7β, and Fbxw7γ (Fig. 2*E*). In the absence of MG132, FLAG(M)-Fbxw7α was localized to the nucleus, FLAG(M)-Fbxw7β was detected at the ER, and FLAG(M)-Fbxw7γ was predominantly nucleolar, consistent with previous findings (3). In the presence of MG132, however, FLAG(M)-Fbxw7α was detected in the cytosol, in addition to the nucleus in some cells, with a high expression level of the protein (Fig. 2*E*, *arrowhead*). Similarly, FLAG(M)-Fbxw7γ was detected in the nucleoplasm in addition to the nucleolus. These results suggested that the interaction between Fbxw7α and the FL forms of OASIS and BBF2H7 detected by coimmunoprecipitation analysis was an artifact of Fbxw7α overexpression and MG132 treatment.

Fbxw7 Controls the Stability of OASIS and BBF2H7—We next examined whether Fbxw7 affects the abundance of OASIS and BBF2H7 in cells. Sustained overexpression of Fbxw7α in HeLa cells resulted in a substantial decrease in the amounts of both OASIS(N) and BBF2H7(N) as well as of the positive controls KLF5 and c-Myc (Fig. 3, *A* and *B*). The abundance of FL forms of OASIS and BBF2H7 at the ER was not affected by overexpression of Fbxw7α. Although RNAi-mediated depletion of Fbxw7 did not affect the abundance of OASIS and BBF2H7 mRNAs (Fig. 3*C*), it resulted in a marked increase in the amounts of OASIS(N) and BBF2H7(N) proteins without substantially affecting the amounts of OASIS(FL) and BBF2H7(FL) (*D* and *E*). Furthermore, cycloheximide chase assays revealed that the half-lives of OASIS(N) and BBF2H7(N) were increased substantially in Fbxw7-depleted cells compared with those in mock-depleted cells (Fig. 3, *F* and *G*).

We also examined whether OASIS(N) and BBF2H7(N) are direct substrates of $SCF^{Fbxw7α}$ *in vitro*. His_6-HA-tagged forms of OASIS(N) and BBF2H7(N) were expressed in and purified from Sf21 insect cells. The purified proteins exhibited multiple bands on Phos-tag SDS-PAGE (Fig. 4*A*), and the lower-mobility

Downloaded from http://www.jbc.org/ at FUZOKU TOSHOKAN KYUSHU UNIV on February 1, 2014

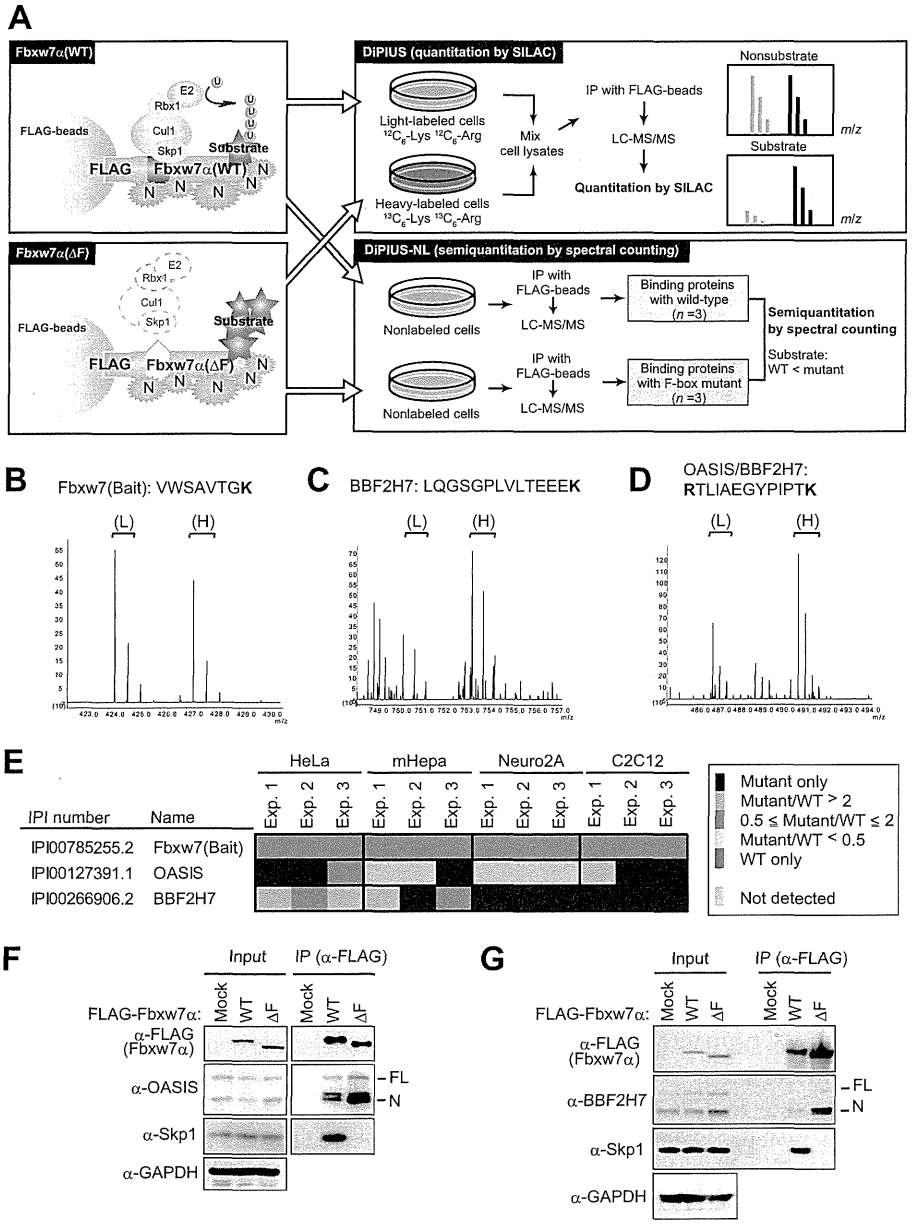


FIGURE 1. **Identification of OASIS and BBF2H7 as candidate substrates of SCF^{Fbxw7} by DiPIUS analyses.** *A*, strategy for comprehensive identification of substrates for Fbxw7α. Schematics of DiPIUS and DiPIUS-NL are shown. Proteins that bind to WT or ΔF mutant forms of Fbxw7α are analyzed by quantitative SILAC (DiPIUS) or semiquantitative spectral counting (DiPIUS-NL). *U*, ubiquitin; *N*, nonspecific binding protein; *IP*, immunoprecipitation. *B–D*, representative mass spectra for DiPIUS analysis of Fbxw7α in mCAT-HeLa cells subjected to SILAC. Peak areas of light (*L*) and heavy (*H*) tryptic peptides derived from Fbxw7 (*bait*) (*B*), BBF2H7 (*C*), or OASIS and BBF2H7 (*D*) represent the abundance of proteins associated with the WT or ΔF mutant forms of Fbxw7α. *E*, OASIS and BBF2H7 were detected by DiPIUS-NL in mCAT-HeLa, mHepa, Neuro2A, or C2C12 cells. The ratios of the number of spectral counts for WT and mutant F-box proteins are indicated by the color scale. Proteins with a mutant/WT ratio of > 2 in at least two of three independent experiments (*Exp.*) were considered binding proteins with a higher affinity for the mutant F-box protein than for the WT protein. *F* and *G*, coimmunoprecipitation of endogenous OASIS (*F*) and BBF2H7 (*G*) as well as of Skp1 with FLAG-tagged WT or ΔF mutant forms of Fbxw7α from mCAT-HeLa cell lysates. Immunoprecipitates (*IP*) prepared with antibodies to FLAG from cells expressing the recombinant Fbxw7α proteins (or from those transfected with the corresponding empty vector, *Mock*) and treated with 10 μM MG132 for 6 h were subjected, together with the original cell lysates (*Input*), to immunoblot analysis with the indicated antibodies (α-).

bands were reduced in intensity after treatment of the proteins with calf intestinal alkaline phosphatase, supporting the notion that the recombinant proteins were phosphorylated. We also expressed His_6-Myc-tagged Skp1, His_6-Myc-tagged Cul1, Myc-tagged Rbx1, and His_6-FLAG-tagged Fbxw7α in Sf21 cells and purified $SCF^{Fbxw7\alpha}$ from the cells with antibodies to FLAG. *In vitro* ubiquitylation assays with these recombinant proteins revealed that the ubiquitylation of OASIS(N) and BBF2H7(N) was apparent only in the presence of all reaction components, including Uba1 (E1), UbcH5C (E2), $SCF^{Fbxw7\alpha}$ (E3), and ubiquitin (Fig. 4, *B* and *C*). We also examined whether full-length recombinant OASIS and BBF2H7 underwent ubiquitylation *in vitro*. Both OASIS(FL)-HA and BBF2H7(FL)-HA were indeed ubiquitylated by $SCF^{Fbxw7\alpha}$ *in vitro* (Fig. 4, *D* and *E*). However, given that the subcellular localization of endogenous full-length OASIS and BBF2H7 differs from that of Fbxw7α under normal conditions (Fig. 2, *D* and *E*), these latter reactions are unlikely to occur *in vivo*. Collectively, these results suggested

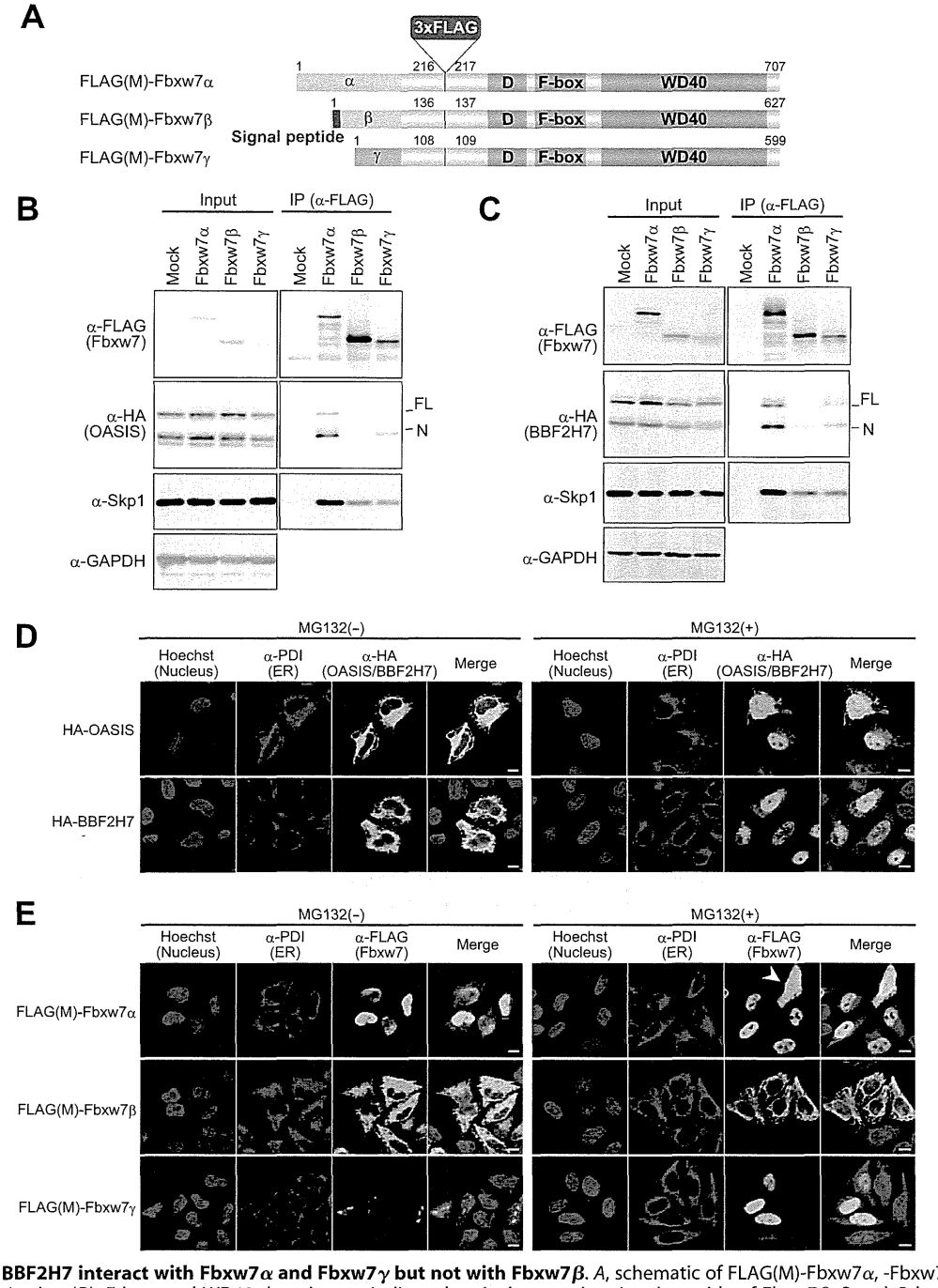


FIGURE 2. **OASIS and BBF2H7 interact with Fbxw7α and Fbxw7γ but not with Fbxw7β.** *A*, schematic of FLAG(M)-Fbxw7α, -Fbxw7β, and -Fbxw7γ. The isoform-specific, dimerization (*D*), F-box, and WD40 domains are indicated, as is the putative signal peptide of Fbxw7β. *B* and *C*, lysates of HEK293T cells expressing FLAG(M)-tagged Fbxw7α, Fbxw7β, or Fbxw7γ together with HA-tagged forms of OASIS (*B*) or BBF2H7 (*C*) were subjected to immunoprecipitation (*IP*) with antibodies to FLAG, and the resulting precipitates were subjected to immunoblot analysis with the indicated antibodies. *D*, mCAT-HeLa cells expressing HA-tagged OASIS or BBF2H7 were incubated in the absence or presence of 10 μM MG132 for 6 h, fixed, and processed for immunofluorescence staining with antibodies to HA (*green*) and protein disulfide isomerase (*PDI*, *red*). Nuclei were stained with Hoechst 33258 (*blue*), and merged images are also shown. *Scale bars* = 10 μm. *E*, mCAT-HeLa cells expressing FLAG(M)-tagged Fbxw7α, Fbxw7β, or Fbxw7γ were incubated in the absence or presence of 10 μM MG132 for 6 h, fixed, and processed for immunofluorescence staining with antibodies to FLAG (*green*) and to protein disulfide isomerase (*red*). Nuclei were stained with Hoechst 33258 (*blue*), and merged images are also shown. The *arrowhead* indicates a cell in which FLAG(M)-Fbxw7α had leaked into the cytosol. *Scale bars* = 10 μm.

that SCF^{Fbxw7} is an authentic ubiquitin ligase for OASIS(N) and BBF2H7(N).

Phosphorylation of OASIS and BBF2H7 Is Necessary for Interaction with Fbxw7—Many substrates of Fbxw7 contain a conserved amino acid sequence for phosphorylation, termed the Cdc4 phosphodegron (CPD) (3). OASIS(N) and BBF2H7(N) each contain an amino acid sequence that matches the CPD, whereas this sequence is not conserved in other CREB3 or CREB3L proteins, including CREBH (CREB3L3), AIbZIP (CREB3L4), and Luman (CREB3) (Fig. 5, *A* and *B*).

To investigate whether the CPD sequence is required for the degradation of OASIS and BBF2H7 dependent on SCF^{Fbxw7}, we

Downloaded from http://www.jbc.org/ at FUZOKU TOSHOKAN KYUSHU UNIV on February 1, 2014